Austrian Journal of Technical and Natural Sciences

№ 9–10 2020
September–October

PREMIER
Publishing

Vienna
2020

Austrian Journal of Technical and Natural Sciences

Scientific journal

№ 9–10 2020 (September–October)

ISSN 2310-5607

Editorial office Premier Publishing s.r.o.
Praha 8 – Karlín, Lyčkovo nám. 508/7, PSČ 18600

E-mail: pub@ppublishing.org

Homepage: ppublishing.org

Austrian Journal of Technical and Natural Sciences is an international, German/English/Russian language, peer-reviewed journal. It is published bi-monthly with circulation of 1000 copies.

The decisive criterion for accepting a manuscript for publication is scientific quality. All research articles published in this journal have undergone a rigorous peer review. Based on initial screening by the editors, each paper is anonymized and reviewed by at least two anonymous referees. Recommending the articles for publishing, the reviewers confirm that in their opinion the submitted article contains important or new scientific results.

Premier Publishing s.r.o. is not responsible for the stylistic content of the article. The responsibility for the stylistic content lies on an author of an article.

Instructions for authors

Full instructions for manuscript preparation and submission can be found through the Premier Publishing s.r.o. home page at:
http://ppublishing.org.

Material disclaimer

The opinions expressed in the conference proceedings do not necessarily reflect those of the Premier Publishing s.r.o., the editor, the editorial board, or the organization to which the authors are affiliated.

Premier Publishing s.r.o. is not responsible for the stylistic content of the article. The responsibility for the stylistic content lies on an author of an article.

Included to the open access repositories:

Typeset in Berling by Ziegler Buchdruckerei, Linz, Austria.
Printed by Premier Publishing s.r.o., Vienna, Austria on acid-free paper.

Section 1. Architecture

https://doi.org/10.29013/AJT-20-9.10-3-5

Kosmii Mykhailo Mykhailovych,
Candidate of Law, Associate Professor, Dean,
Faculty of Architecture, Construction and Design
King Danylo University
E-mail: mykhailo.kosmii@ukd.edu.ua

TRANSFORMATION, HARMONY AND DEGRADATION OF SPACE UNDER THE INFLUENCE OF THE INTANGIBLE FACTOR

Abstract. The article characterizes and analyzes the processes of transformation, harmonization and degradation of spatial structures of settlements under the influence of the intangible factor. The intangible is implemented based on the balance between harmony, consensus and perspective, which naturally leads to the transformation of the spatial structure of cities and territories.

Keywords: transformation, harmony, harmonization, degradation, spatial structure, intangible factor.

Theoretical and methodological study of the phenomenon of the intangible proves that its existence in the spatial structure is natural, and the impact on its development and transformation is determined by a set of external and internal factors present in the city itself. In addition, certain intangible factors, such as legislative and regulatory, property relations or political and administrative ones, are systemically important and determine the nature of the spatial transformation of a particular urban system.

Considering the influence of the intangible on the spatial structure, we should begin with the study of their formal features. Thus, the process of evolution of the architectural form led to the formation of a set of forms that created a separate space with a clear organizational order, requirements and even its own "soul". The city became this new formation. The concept of "city" seems to be clear, but there is no established approach and criteria for its definition. The most common is the opposition of city vs. village. In fact, this approach is of historical origin, but it is limited by the fact that the rapid growth of cities leads to urbanization, and the city transforms from a center of culture, spirituality and ideal space (it maintained this status until the Industrial Revolution) into an environment to meet the functional needs of human activity. It should be noted that both the city and the village develop on a parallel track, but they are closely connected. On the one hand, the village is a source for the development of the city. On the other hand, it is an example of effective transformation of the spatial structure with regard to aesthetic, ethical, environmental, moral and ethical factors, which were traditional in the 21st century. The latter are an expression of the intangible, and therefore evidence of the need to find theoretical and methodological foundations for their consideration in the process of architectural and urban planning.

The influence of the intangible on the spatial structure leads to the transformation or degradation of space. In any case, these diametrically opposed

categories provide for development. However, if the first one leads to harmonization of space, the second one, being effective at a particular time, does not have time perspective.

Urban space is a broad concept based on the understanding of space as a location of people and concentration of their social and household needs, so that the transformation of space as the place for anyone into the space for every person happens at the time of person's impact on the design of urban space.

On the other hand, not every urban space is suitable for creativity, as well. Therefore, it should also be organized with regard to the potential of that "creative stratum of the population", that will change it. This wording leads to a situation in which there is a chance for developing for cities with an active group of people who are ready to change the space around them, has the chance for developing. This group lays the potential and forms the basis for the transformation of urban space not only as the place of residence, but also as the place of development. Perfectly organized urban space is the precondition for further development of the city. Another important component in the process of such transformation is the system of values that begin to dominate in urban planning and define strategies of the urban development. An opportunity for self-realization has always been the main value of urban creativity culture [3, P. 129].

Based on the content of intangible factors, it is advisable to determine concepts, which allow measuring the level of their impact on urban systems. Thus, the concept of "transformation" implies change that has a clear purpose and objectives. It means that this is a solely positive change aimed at improving of the existing space. In the case of urban space, its transformation under the influence of the intangible occurs constantly, and the residents do not always perceive it as a change. Since the intangible possesses a semantic meaning, the transformation of the urban space is expected, but in our opinion, tracking and providing the intangible with quantitative expressions will form a qualitative model of urban development under the influence of the intangible. Modern Ukrainian researchers point at inconsistency and disorder of transformation types because such concepts as modernization, modification, renovation, optimization and others exist at the same time [6, P. 203]. Approaches to the concept of "transformation" used by such Ukrainian scholars as H. Osychenko [4], A. Pleshkanovska [5], V. Timokhin [7] demonstrate differences in the views of historians and architecture theorists, and practitioners as well. There is an interesting research on the ideological transformation of the image of an architectural object by L. Bachynska [1, p. 43–44]. The researcher's argument is the thesis that a person is a consumer of architectural form and urban space, and the ideology with its intangible nature stands out as a link between ordinary consumers and professional architects who are the creators of space [1, P. 44]. We consider "transformation" as a process of qualitative change in the urban space which is the result of the combination of tangible and intangible factors, and it could be directed towards achieving harmony if there is a clear model of development.

In architectural studies, a clear and directed space transformation is classified as harmonization, which proves again that the influence of the intangible on the spatial structure leads to its transformation towards harmonious space. Harmony provides for the combination of heterogeneous or even opposite elements into a single system. Accordingly, a search for harmony in the process of organizing the spatial structure of urban systems is natural in a combination of tangible and intangible.

In architecture it is accepted to use the concept of "harmonization", the basic principles of which include 1) the ability to create the image of the city; 2) compactness; 3) scale; 4) safety; 5) comfort [2, P. 21]. Those principles correspond with the tangible factors, while the intangible forms the harmony of perception of space by the person living in it. Harmony of perception is formed historically under the influence of cultural, ethical and spiritual factors. In our study, the concept of harmony is associated with

the concept of "city brand", because only when the city is harmonious and comfortable for human life, the latter promotes it, forms its semantic image and brand.

The opposite to the concept of harmony is disharmony, which results in the degradation of the spatial structure. It is significant that the disharmony or degradation of space can take place in not only the absence of several tangible or intangible factors, but also when one of them is above the others.

In general, the theoretical features of the intangible and its impact on the spatial structure are: 1) belief in the ability to ennoble man and change his essence; 2) a daily life of people determines their consciousness, and if something bad happens to a person's consciousness, it is the fault of the environment they live in; 3) the space of a city or village can be changed in such way as to change people and communities; 4) historical patterns and corresponding cycles of history are rejected, despite that having understood them would provide the possibility to predict the future and to create it in the corresponding way; 5) urban projects become orthodox, detailed, and do not allow deviations from "the only right" way; 6) the total order and means of its achievement should be provided; 7) individual space disappears, and the city becomes a common space.

Thus, the intangible is much wider and more important than the tangible, since it forms the image of the city, determines its history, reflects the relationship with society, memory, science, art, and more. The image of the city creates first its spiritual and scientific life, it forms its cultural, artistic and intellectual states, a certain level of quality of the social dimension, namely the aspirations and needs of the residents, culture and art, consciousness and language. The transformation of space leads to the harmonization of architectural objects, but the avoidance of individual components or the dominance of the tangible has the effect of establishing disharmony.

References:

1. Bachynska L. H. Ideolohichna transformatsiia obraza arkhitekturnoho obiekta yak vidobrazhennia dynamiky suspilno-politychnykh umov. International Scientific and Practical Conference World science, 2017. – No. 1. P. 43–52.
2. Korotun I. V. Osnovy harmonizatsii arkhitekturnoho seredovyshcha. Visnyk Natsionalnoho universytetu "Lvivska politekhnika". Arkhitektura. 2014. – No. 793. P. 19–26. URL: http://nbuv.gov.ua/UJRN/VNULPARX_2014_793_8.
3. Moiseev Yu. M. Porogi neopredelennosti v sisteme gradostroitelnogo planirovaniya. Dissertatsiya na soiskanie uchenoy stepeni doktora arhitekturyi. 05.23.22 Gradostroitelstvo, planirovka selskih naselennyih punktov. M., 2017. – 345 p. URL: https://marhi.ru/sciense/author/moiseev/moiseev_v1_21_09_2017.pdf.
4. Osychenko H. O. Rekonstruktsiia istorychnoho seredovyshcha mista. Mistobuduvannia ta terytorialne planuvannia. 2009. – Vyp. 35. – P. 343–354.
5. Pleshkanovska A. M. Metodolohiia kompleksnoi rekonstruktsii mista. Avtoref. dys. na zdobuttia nauk. stupenia d-ra tekhn. nauk: 05.23.20. – Kyiv, 2013. – 40 p.
6. Stetsiuk I. I. Typy ta vydy harmoniinoi transformatsii miskoho seredovyshcha. Suchasni problemy arkhitektury ta mistobuduvannia. 2015. – Vyp. 41. – P. 203–208.
7. Timokhin V. Problemy i pryntsypy rekonstruktsii suchasnoho miskoho seredovyshcha. Dosvid ta perspektyvy rozvytku mist Ukrainy. 2014. – Vyp. 26. – P. 15–25. Rezhym dostupu: URL: http://nbuv.gov.ua/UJRN/dprmu_2014_26_4.

Section 2. Biology

https://doi.org/10.29013/AJT-20-9.10-6-10

Mardomi Farid Davoud,
doctoral student at the Department of Genetics
and Evolutionary Doctrine Baku State Universitye
E-mail: mardomi.farid@mail.ru

Deljavan-Nikouei Forough Hassan,
doctoral student at the Department of Genetics
and Evolutionary Doctrine Baku State University
E-mail: deljavan@mail.ru

Babayev Medjnun Shikbaba,
Doctor of Biological Sciences, Professor of the Department
of Genetics and Evolutionary Doctrine Baku State Universitye
E-mail: babayev_1940@mail.ru

MAIN TRENDS OF THE GENETIC FACTOR OF MALE INFERTILITY

Abstract. For centuries, male infertility and problems with impaired fertility have been a problem around the world. It is also a serious clinical problem today, which affects 8–12% of couples worldwide. Of all cases of infertility, approximately 40–50% are associated with "male factor" infertility, and up to 2% of all men show sub-optimal sperm parameters. It can be one or a combination of low sperm concentration, poor motility, or abnormal morphology. Our review will help to find out some of the trends in male infertility and to elucidate in the future various factors that may be responsible for this pathology.

Keywords: male infertility, fertility, sperm, diagnostics, deletions, genes, mutation.

Introduction

Male infertility (MI) is a serious pathological condition that requires a comprehensive comprehensive diagnosis, urgent correction, and in some cases prevention. Infertility affects 15–20% of couples of reproductive age. In half of the cases, it is associated with the "male factor", manifested by deviations in the parameters of the ejaculate [1, p. 191–196].

The complexity of diagnosing male infertility is due to the large number of reasons that cause it. These include anomalies of the genitourinary system, tumors, infections of the genitourinary tract, endocrine disorders, immunological factors, genetic mutations, etc. In contrast to the above reasons, genetic ones do not always have clinical manifestations, but are extremely important for the diagnosis of MI in the subject. It is important to understand that the diagnosis of "MI" and its forms can only be made by a specialist doctor on the basis of anamnestic data, examination data, results of instrumental and labora-

tory studies [2, p. 9–16]. The following reasons may be the reason for going to the doctor:

- impossibility of conceiving a child within a year, provided that there are no signs of female infertility in the partner;
- violations of erectile and ejaculatory functions;
- concomitant diseases of the urogenital sphere (inflammatory, tumor, autoimmune, congenital, etc.);
- taking hormonal and cytostatic drugs;
- discomfort in the urogenital area.

Genetic causes of male infertility

Frequent causes of male infertility are disorders in the structure and number of sperm, which affect their mobility and ability to fertilize.

The main genetic causes of male infertility development are:

1) deletion (removal of genetic fragments) of the AZF locus;

2) polymorphism (increased repeats of the genetic fragment – CAG) of the androgen receptor (AR) gene;

3) mutations (sequence disruption) of the CFTR gene.

Currently, these markers are an integral part of the standard criteria for the complex diagnosis of genetic manifestations of male infertility, occurring in a group of patients in 10–15% of cases [3, p. 28–30].

Deletions of the AZF locus and the SRY gene

An important role in the development of pathologies such as oligozoospermia and azoospermia is played by deviations in a specific region of the Y chromosome – the AZF locus (azoospermia factor). The genes included in it determine the normal course of spermatogenesis, and if the genetic structure of the AZF locus is disrupted, the formation of male germ cells can be seriously impaired.

The AZF locus is located on the long arm of the Y chromosome (Yq11). The genes located at this locus play an important role in the process of spermatogenesis. Microdeletion of the Y chromosome is the loss of certain areas, is found on average in 10–15% of cases of azoospermia and in 5–10% of cases of severe oligozoospermia and causes impaired spermatogenesis and infertility in men [4, p. 218–220].

The AZF locus is divided into 3 sections: AZFa, AZFb and AZFc. In each of them, genes involved in the control of spermatogenesis have been identified. Deletions at the AZF locus can be complete, i.e. completely removing one of the AZF regions or more, and partial, when they do not completely cover any of its three regions.

With complete AZF deletions, there is a fairly clear dependence of the degree of spermatogenesis impairment on the size and location of the deletions, which may have a prognostic value in obtaining spermatozoa suitable for in vitro fertilization programs. The absence of the entire AZF locus, as well as deletions that completely cover the AZFa and / or AZFb regions, indicate the impossibility of obtaining spermatozoa.

Almost all patients with AZFb or AZFb + c deletions have azoospermia due to severe spermatogenesis disorders (Sertoli cell only syndrome). With complete deletions of the AZFc region, manifestations range from azoospermia to oligozoospermia. On average, in 50–70% of patients with a deletion that completely captures the AZFc region, it is possible to obtain spermatozoa suitable for artificial insemination. With partial AZF deletions, manifestations range from azoospermia to normozoospermia [5, p. 80–87].

Investigation of the state of the AZF locus of the Y chromosome in patients with azoospermia and severe oligozoospermia makes it possible to establish the genetic cause of spermatogenesis disorders, to carry out differential diagnostics of infertility in men and to adjust the treatment, to check the possibility of obtaining spermatozoa with testicular biopsy and the possibility of obtaining spermatozoa for ICSI (intracytoplasmic injection).

It should be borne in mind that in the case of successful use of assisted reproductive technologies, the deletion of the Y chromosome is transmit-

ted through the male line. This shows the need for dispensary observation of boys born after the use of ICSI in fathers with microdeletions in the Y chromosome in order to assess their fertile status. Indications for AZF deletions are based on sperm count and include azoospermia and severe oligozoospermia (<5 million sperm / ml ejaculate).

The SRY gene (Sex-determining Region Y) is especially important in the genetic control of male development. It was in it that the largest number of mutations associated with gonadal dysgenesis and / or sex reversal was found. In the absence of a chromosome region containing the SRY gene, the phenotype will be female with a male karyotype of 46XY. This genetic study includes the analysis of the AZF locus of the chromosome – 13 clinically significant deletions: sY86, sY84, sY615, sY127, sY134, sY142, sY1197, sY254, sY255, sY1291, sY1125, sY1206, sY242, as well as determination of the SRY gene deletion.

Androgen receptor gene (AR)

Another determining factor in male infertility is a violation of the hormonal regulation of spermatogenesis, in which male sex hormones androgens play a key role. They interact with specific androgen receptors, determining the development of male sexual characteristics and activating spermatogenesis. Receptors are found in cells of the testes, prostate, skin, cells of the nervous system and other tissues. The androgen receptor gene is characterized by the presence of a sequence of CAG (cytosine-adenine-guanine) repeats, the number of which can vary significantly (from 8 to 25). The CAG triplet encodes the amino acid glutamine, and when the number of CAG repeats of nucleotides changes, the amount of the amino acid glutamine in the protein also changes. The sensitivity of the receptor to testosterone depends on the number of repeats in the AR gene, and the relationship is inversely proportional: the more repeats, the less sensitive the receptor. An increase in the number of CAG repeats in receptors reduces their activity, they become less sensitive to testosterone, which can lead to impaired spermatogenesis, and the risk of developing oligozoospermia and azoospermia increases [6, p. 122–123].

There is also evidence that with a reduced number of CAG repeats (<18) in the AR gene, there is an increased sensitivity to androgens and an increased risk of prostate cancer in men. An increase in the number of CAG repeats up to 38–62 leads to spinbulbar muscle atrophy, Kennedy type. The test result makes it possible to assess the activity of spermatogenesis and, if necessary, take appropriate measures to compensate for the pathology.

Male infertility with cystic fibrosis

Cystic fibrosis (synonymous with cystic fibrosis) (CF) is one of the most common autosomal recessive hereditary diseases in humans. It is characterized by dysfunction of the epithelium of the respiratory tract, intestines, pancreas, sweat and sex glands. Cystic fibrosis is caused by mutations in the cystic fibrosis transmembrane regulator (CFTR) gene, which encodes an ATP-binding protein that forms a channel for chlorine ions in the cell walls. Mutations lead to a disruption in the transport of electrolytes and chlorine ions across the membranes of epithelial cells, which is accompanied by increased secretion of thick mucus and blockage of the excretory ducts of various glands. In 98% of men with cystic fibrosis, reproductive function is impaired, as there is azoospermia or severe oligozoospermia (less than 5 million sperm in 1 ml of semen) [7, p. 226–239].

The membrane protein encoded by the CFTR gene functions as an ion channel while simultaneously influencing the formation of the ejaculatory ducts, seminal vesicles, vas deferens, and distal 2/3 of the epididymis. Due to the mutation, the transfer of chlorine through the channels to the cells that produce mucous secretions is disrupted. This is the reason for the dehydration of the secretion, it becomes thicker and more viscous.

In men with cystic fibrosis, the vas deferens are most often absent or blocked by a plug of thick mucus. Moreover, the disease does not interfere with the production of sex hormones and the function

of the gonads. Sexual development is normal, although it can be slowed down by pulmonary disease and poor digestion.

A mutation in the CFTR gene is associated with congenital bilateral absence of the vas deferens (CBAD). In some men, it is the congenital absence of both vas deferens that is the only symptom of the disease, or there are moderate clinical manifestations of cystic fibrosis (for example, a history of frequent infections with lung damage). Because the vas deferens in most men with CF is absent or not functional, sperm cannot pass through them. As a result, although the testes produce these cells, the sperm does not contain them. New technologies of in vitro fertilization (IVF / ICSI) allow many men with CF to have children, and in some sick men the ducts are still present and not blocked [8, p. 47–58].

The absence of the vas deferens is often undetectable, so all patients with azoospermia should be examined very carefully to rule out CBAD. Patients diagnosed with CBAD need to undergo CFTR gene analysis. Mutations can be found in both copies of the CFTR gene, however, in most men with CBAD, the mutation is found in only one allele. In such presumably heterozygous cases of carriage, an unknown or rare 2nd mutation may be present.

If a CFTR gene mutation is detected in a man during family planning, it is important to conduct molecular genetic testing of the partner. According to statistics, in the European population, on average, every 25th person is a carrier of CFTR gene mutations. If a woman and a man are carriers of the CFTR gene mutation, the probability of having a child with cystic fibrosis will be 25%.

If one of the future parents is sick with cystic fibrosis, and the other is a carrier, then the probability of having a child with cystic fibrosis will be 50%. In the remaining 50% of cases, he will be a clinically healthy carrier of the disease. If one parent has cystic fibrosis and the other is neither sick nor carrier, then all children will be clinically healthy carriers of the disease. However, in the future, they and their partners may need genetic counseling to predict the birth of sick children in the next generation. If both parents are diagnosed with cystic fibrosis, then the child will inevitably be sick. In all cases of mutation carriage, medical genetic counseling is recommended for family planning [9, p. 324–332].

Conclusion

Successful treatment of infertility by methods of assisted reproductive technologies has led to the emergence of a new problem – obtaining healthy offspring. A necessary stage in the treatment of infertility should be medical and genetic counseling, on the basis of which the doctor receives information about the need for genetic research of a married couple.

Thus, the analysis of literature data indicates that in our time the diagnosis of male infertility is at a high level and there are many modern, high-tech ways of diagnosis and therapy. We can say with confidence that genetic analysis can identify up to 95% of all possible patients. The totality of the results that can be obtained during genetic testing for the presence of AZF deletions in a man, determination of the number of CAG repeats of the AR gene and mutations in the CFTR gene makes it possible to identify problems in the male line when planning pregnancy, make a decision on the tactics of patient management and, if necessary, choose the optimal scheme of assisted reproductive technologies (ART) [6, p. 122–123].

References:

1. Naina Kumar and Amit Kant Singh Trends of male factor infertility, an important cause of infertility: A review of literature J Hum Reprod Sci. Oct-Dec; 2015.– 8(4). – P. 191–196.
2. Dabaja A. A., Schlegel P. N. Medical treatment of maleinfertility. Transl Androl Urol,2014.– 3(1). – P. 9–16.

3. Fedorova N. I. and coauthors. The value of embryonic cells isolated from the cervical canal in early non-invasive prenatal diagnosis. Obstetrics and gynecology.2010. – No. 1. – P. 28–30.
4. Radchenko OR Risk factors of male infertility and methods of prevention // Practical medicine.– No. 57. 2012.– P. 218–220.
5. Lyzikova Yu. A. Assisted reproductive technologies in the treatment of infertility. Protection of motherhood and childhood.2010. – No. 2–16. – P. 80–87.
6. Gordeeva V. L., Togobetsky A. S., Kulikova O. R. The use of ART for severe forms of male infertility. Reproductive technologies today and tomorrow. Materials of the XXI International Conference of the Russian Association of Human Reproduction.– St. Petersburg, 2011.– P. 122–123.
7. Foresta C., Moro E., Ferlin A. Y chromosome microdeletions and alterations ofspermatogenesis. Endocr Rev.2001.– 22(2). – P. 226–239. DOI:10.1210/ edrv.22.2.0425
8. Chernykh V. B., Kurilo L. F., Polyakov A. V. Y chromosome, AZF microdeletions and idiopathic infertility in men, Reproduction problems.2001. – 5(7). – P. 47–58.
9. Jungwirth A., Giwercman A., Tournaye H., Diemer T., Kopa Z., Dohle G., et al. Guidelines on Male Infertility. Eur Assoc Urol.2012.– 62 (2). – P. 324–332. DOI: 10.1016/j.eururo.2012.04.048

Section 3. Biotechnology

https://doi.org/10.29013/AJT-20-9.10-11-22

Lolakhon Ettibaeva,
Senior Teacher of the Department of Chemistry at Gulistan State University
E-mail: lola1981a@mail.ru
Abdurakhmanova Ugiloy,
Head of the Department of Chemistry at Gulistan State University
E-mail: ugi_lay-912@mail.ru
Boburjon Yusupov,
Master of chemistry department
Makhammadiev Sharoffiddin,
Master of chemistry department
Faculty of Natural Science, Gulistan State University, Uzbekistan

ACQUISITION OF SUPRAMOLECULAR COMPLEX OF GLITSIRRIZIN ACID WITH MENTHOL AND THEIR CHEMICAL IDENTIFICATION

Abstract. In this study, the supramolecular complexes were obtained from glycyrrhizic acid (GA) and Menthol (1R, 2S, 5R) –2-isopropyl-5-methylcyclogeksanol) with various ratios. It has been shown the highest yield of the supramolecular complex with GA and Menthol in a 4:1 (GA: Menthol) ratio. This combination has been chemically identified by comparing the IR-Fure spectra of the initial agents. Similarity coefficients of the initial agents for the supramolecular complex GA: Menthol (4:1) showed as a 0.84 and 0.70 coefficient with known functional groups of GA.

Keywords: Glycyrrhiza glabra L., glycyrrhizic acid, menthol, supramolecular complex, IR spectroscopy.

Introduction

Glycyrrhizic acid (GA) (20 β-carboxy-11-oxo-30-norolean-12-en-3 β-il-2-O-β-D-glucopyranuronosyl-α-D-glucopyranose-duronic acid) is a valuable raw material, which is important in the food industry, cosmetology, and other industries. Based on the chemical structure of glycyrrhizic acid, it is a glycoside, which is formed by glucuronic acid residue with triterpene-glycyrrhizic acid [1–2] (Figure 1 A). Many studies on the physical-chemical features of GA showed the molecule contains hydrophobic (triterpene fragment) and hydrophilic (two glucuronide residues) parts that are assumed to make a mycelium in the complexes [3–4].

The GA is extracted from the root of licorice (*Glycyrrhiza glabra L.* and *Glycyrrhiza uralica L.*) [5]. Several compounds of GA were obtained and used for various purposes. The GA can be easily formed with other molecules to make a supramolecular compound called a "*guest-host*" type [6]. Other studies

were also confirmed that GA provides a "host-guest" type of auto association [7–9].

The supramolecular complex of GA is characterized as a ring dimer structure with hydrophobic cavities due to intermolecular hydrogen bonds. This cavity can provide a "*guest-host*" type formation [10].

The GA reacts with many other molecules to yield a supramolecular complex [11–15]. Particularly, increasing GA concentration stimulated the auto association of the "guest-host" type of supramolecular complex with streptomycin under the various ratio of GA: streptomycin (1:1, 2:1, 3:1, 3:2) [16].

At present, a lot of supramolecular complexes based GA with various agents were chemically synthesized and used in various fields. For instance, before sowing wheat seed treated GA and its denatured salt combined with "Tebukonazol" enhanced the resistance to various pathogenic infections at the early stage of plant organogenesis and increased yield productivity [9]. It is assumed that GA molecules (~60–100) form vesicles/mycelium and provide increased transmembrane penetration with the main drug molecules involved [9].

The therapeutic dosage of some medicines can often cause adverse effects [17–18]. It is worth noting that positive results are obtained based on the use of supramolecular compounds of GA. For example, a supramolecular complex of GA and streptomycin can reduce the dose of the drug used [19–20]. Supramolecular complexes are used in practice as an effective method of increasing the water solubility level of pharmacological preparations based on mechanical and chemical mechanisms. In particular, studies have shown a significant increase in the solubility levels of drugs such as Diazepam (Sibazon), "Nifedipine", "Ibuprofen". It is assumed that this is due to the physicochemical properties of the micelles that form the GA molecule [9].

Menthol ($C_{10}H_{20}O$) is a terpenoid that found in the essential oils of the mint family (Mentha sp.). It is a white crystalline solid that can dissolve well at room temperature or partially at high temperatures. There are several isomers of menthol including isomenthol, neomenthol, neo-isomenthol with peppermint odor. Among them, (–) menthol (1R, 2S, 5R)-2-isopropyl-5-methylcyclohexaneanol) is one of the strong aromatic molecules in nature (Figure 1 B).

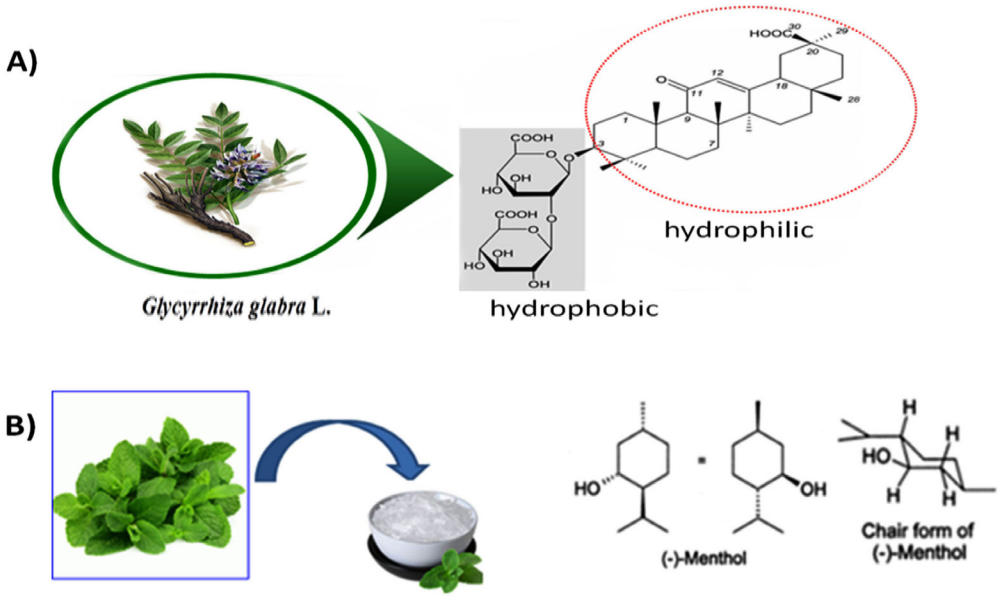

Figure 1. Molecular structures of glycyrrhizic acid (GA) and Menthol. (A) Glycyrrhizic acid (Empirical formula – $C_{42}H_{62}O_{16}$; 20β -carboxy-11-oxo-30-norolean-12-en-3 β-il-2-O- β -D-glucopyranuronosyl-α-D-glucopyranose-duronic acid) [2]; (B) Menthol ($C_{10}H_{20}O$);

The (–) Menthol is a known with strong cooling and refreshing agent and four times higher efficacy than (+) menthol isomers [21]. Therefore, some of its derivatives are widely used in medicine, pharmaceutics, perfumery and food industries. Menthol cools the skin when it applied to the skin; therefore it is used as a medicine during the headache. Moreover, (–) menthol can also use as antiseptic properties to nose and throat mucus [22]. Nowadays, one of the crucial tasks in agriculture involves the enhancing of plant productivity with sustainable chemicals. In the present research, the GA was extracted from the licorice root and synthesized it's a supramolecular complex with menthol.

Main Part

Materials and methods

The spectrophotometric methods for quantitative/qualitative chemical identification of GA in biomaterial content are used effectively [23–26]. Some researchers have noted the efficacy of *Glycyrrhiza glabra L.* root mass extraction in high-temperature aqueous environments, in the next step, the formation of low concentrations in a vacuum apparatus, HNO_3 solution (3%) and extraction of GA based on acetone extracting [27]. Another study used an NH_4OH (1%) for the extraction of GA from the root of the licorice. In case, the acid was removed by H_2SO_4 solution [28].

Extraction of GA. Some methods are available to extraction and chemical identification for the GA from licorice (*Glycyrrhiza glabra L.)* root [29]. We have used a local licorice root from a Sirdarya region, Uzbekistan. Approximately 100mg which is 92% technical GA dissolved with 3% Sulphate acid and boiled in a water bath until to get a white powder. After then this product was cooled at room temperature overnight. The contents then were filtered with filter paper and washed with cold distilled water. Final extract dried and stored in a dark condition for further experiment. Purity: 92%, Tliq = 210–213 ˚C / a / D25 = =+48 (dis.water. Ethanol 1: 1); Rf = 0.83 (1), Yield: 98%. IR spectra: 1041 cm^{-1} ($-O^-$); 1656 cm^{-1} (CO); 2873 cm^{-1} (CH_3); 3247 cm^{-1} (OH).

Identification of GA. Chemical identification of GA was performed by using standard methods which are mentioned in some reference [30–31]. In our experiments, root extract was analyzed by using a Perkin Elmer Spectrum IR (Germany; version 10.6.1) IR-Fure spectrometer in the range of 4000––500 cm^{-1}. KBr tablet was used as a standard GA for the preparation of test samples. The IR spectra of GA and β-indolyl-3-acetic acid were compared with the spectra of the "Biochemica" Biblioteca.

Obtaining a supramolecular complex.

Supramolecular compounds were obtained by the following steps. Firstly, 1.68 g (0.002 M) of GAMAT dissolved 25 ml distilled water and 25 ml ethanol. This solution widely mixed with a magnetic stirrer at 50–60 ˚C. Then we added 0.156 g (0.001 M) Menthol and continued the mixing process for 5–6 hours. After then the reaction mixture was filtered. The rest of the ethanol was removed in a vacuum, and the aqueous part was dried in a lyophilic manner. Final product was a yellow powder: liquid=205–210 ˚C Rf = = 0.9 (System 2) Units: 85% IR spectrum:1042 ($-O^-$) cm^{-1}; 1655 (CO) cm^{-1} 2948 (CH_3) cm^{-1}; 3600–3200 (OH) cm^{-1}. Other supramolecular complexes of GA with Mt were also obtained by this synthesis method:

1. GA: MT (2: 1). Liquid = 218–220 ˚C Rf= 0.8 (System 2) Productivity 95%

2. GA: MT (4: 1). Liquid = 220–225 ˚C, Rf (1) Productivity: 90%.

Reagents and equipment. In our experiment, we have used ethanol, benzene, acetone acid solutions, as well as alkaline solutions as organic solvents for dissolving. The Chromatography (TLC) was used for thick layer:

1) benzine: acetone 5:3,

2) acetonitrile: water 1:2,

3) benzine -ether 15:3;

4) benzine: acetone 5:1

5) acetone: Alcohol is treated with 1: 1.

10% alcohol solution of sulfuric acid (H_2SO_4) and iodine chamber for chromatography staining were monitored.

Continuously stirring was performed by using a magnetic mixer MM-5 TU25-11834-80. The organic solvent was evaporated from the system on an IR-1M2 rotor evaporator. For drying we have used the Automatic FREEZE-Dryer10-010, a lyophilic device and a PTP TU25-11-1144 unit were used to measure the fluid temperature of the substances. The structure of supramolecular complexes was performed on the IR spectrometer FT-IR System-2000. The Silufol (Czech Republic) plates were used for thin-layer chromatography.

Preparation of a working standard solution for glycyrrhizic acid: 0.10 precise drawer was weighed on analytical weight and placed in a 100ml measuring tube. 10 ml 96% ethanol was added, diluted thoroughly and filled with distilled water to the measuring line (Solution A). After thoroughly shaking the tube, 1 ml of aliquots were taken and diluted with 9 ml. fluid system (Solution B, working standard solution), 0.1 mg/ml. The standard working solution was placed on a chromatograph for analysis.

Preparation of the solvent system: 14 ml of acetonitrile and 0.5 ml of acetic acid and water-filled till 50 ml tube. This solution (pH 3.0–3–5) always used in our work.

Results and discussion

Currently, modern physic-chemical methods are available for GA extraction including boiling of root tissue at high-temperature water [27; 32], NaOH aqueous solution [33], methanol [34], ethanol [35–36], and the use of ammonia solutions. As well as, the vacuum-pulse methods [33], ultrasound [37] also used to increase the efficiency of extraction.

In our experiment, local licorice (Glycyrrhiza glabra L.) roots were washed with distilled water and dried. Then the roots were mechanically milled to < 0.5 – 1 mm size. Extra agents were selected according to the literature data [38]. Firstly, pieces of the roots were cracked in 70% ethanol at 1:5 ratios and kept in dark for 5 days that stirring constantly. In the next step, the extract was filtered and the ethanol was evaporated under + 75 °C [39]. The mass column (h = 20 cm; ø = 2.5 cm) was divided into fractions (3) by using a chromatography. The elution was carried out in 1% ethanol (75%) of the ammonia solution. The fractions were analyzed by using high-performance liquid chromatography 1200 series DAD detector with Agilent Technologies (USA), high-performance liquid chromatography (150 × 4.6 mm); 5 μm) at +20 °C. The flow rate value of the moving phase shows a 0.5 ml/min. The methanol and an acidic acid solution (0.05%) were used as the active phase. Detection was carried out in the250 nm, 275 nm, and 350 nm full-length sectors. As a standard sample, we have used ammonium salts of GA (Sigma-Aldrich, Germany). In results, the higher concentration of the GA can observe at a second fraction (Table 1).

Table 1. – Quantification of GA from root tissue extract of the licorice (*Glycyrrhiza glabra L.*)

Fractions	Concentration (in accordance with dry specimen, mg/g)	Weight share (%)
1	2.4	0.24
2	5.8	0.65
3	3.6	0.38

Our next experiment was root biomass (5 ± ± 0.5 g) of licorice (*Glycyrrhiza glabra L.*) was mixed with dilution (distilled water+ammonia solution (3%); +150 °C; 5 MPa) at a ratio of 1:10. The prepared extagent in the tube for 120 min continued boil and cooled and filtered. The method was used to determine the amount of GA in the extract. Acetonitrile+methanol+distilled water+acetic acid (35 : 20 : 45 : 1) was used as an active phase (flow rate 0.5 cm/min). Detection was performed at a wavelength of 256 nm (Table 2).

It reported that the GA content from aqueous extract is a 13.6% [32] compared to the dry plant mass, a 7.3% [38] in some data, and 0.88% in ethanol extract [35], and also when used ultra-sound, it was found to be 3.64% [37].

Synthesis and chemical identification of supramolecular complex of glycyrrhizic acid with menthol.

The supramolecular complex of GA with menthol was obtained according to (Scheme 1).

Table 2.– GA content in *Glycyrrhiza glabra L.* root extract (n = 3 – 5)

Conditions of extradiction	Identification through gravimetric method			Identification through HPLS	
	Quantity in water extract (%)	Quantity in filtered content (%)	Quantity in accordance to dry plant mass (%)	Concentration in extract (mg/ml)	Share in extract content (%)
Distilled water + ammonia solution (3%); +150 °C; 5 MPa	0.074 ± 0.005	0.083 ± 0.04	14.3 ± 0.28	7.75 ± 0.3	0.9 ± 0.04

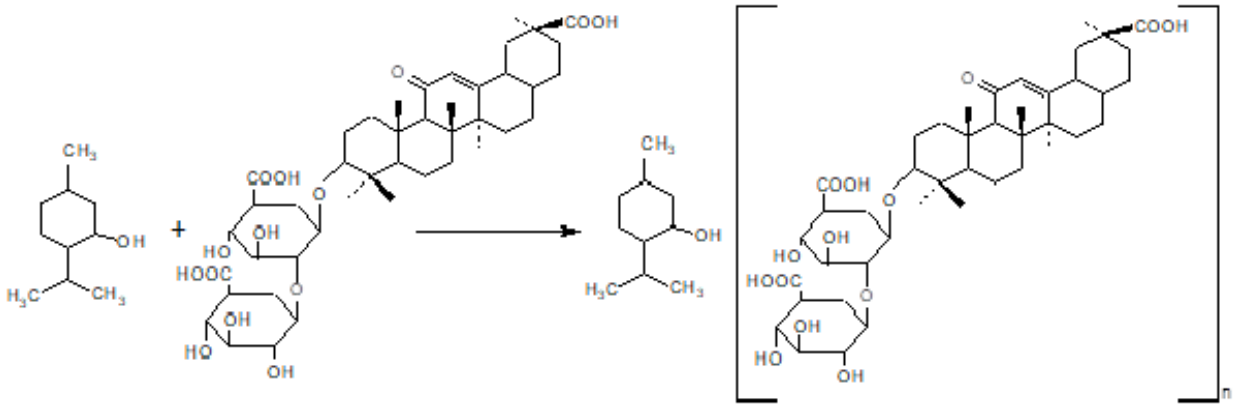

Scheme 1. Reaction of the supramolecular complex between GA and Menthol

Supramolecular complexes with molar ratio 2:1; 4:1; 9:1 of glycyrrhizic acid with menthol were obtained in water: acetone system.

Some physical-chemical properties of the resulting supramolecular compounds were studied and their chemical structures were investigated by IR spectroscopy (Table 3).

Table 3.– Some physical-chemical descriptions of supramolecular complex of GA with menthol

No.	Substances	T_{liquid}, °C	$R^{*}_{f\ (system)}$	Solubility	IR spectrum, cm^{-1}
1	GA: Menthol 2:1	218–220 °C	0.8	Water alcohol	3400–3500(OH); 2924(CH_3) 2857–(CH_2); 1637–1725–(CO) 1085–($-O^-$)
2	GA: Menthol 4:1	220–225 °C	0.9	Water alcohol	3400–3500(OH); 2924(CH_3) 2857–(CH_2); 1637–1725-(CO) 1085-($-O^-$)
3	GA: Menthol 9:1	228–230 °C	0.8	Water alcohol	3400–3500(OH); 2924(CH_3) 2857–(CH_2); 1637–1725–(CO) 1085–($-O^-$)

As shown in (Table 3), all obtained complex compounds are well soluble in water. It can be seen that the liquid temperature is between 200 and 230 ˚C.

System: benzine: chloroform 3:1

The structure of the supramolecular complex was studied by physical methods based on the interaction of organic molecules with electromagnetic radiation, in particular their IR spectrum (the frequency of vibration of atoms in the molecule, $\lambda = 10^{-4} - 10^{-2}\ cm^{-1}$).

The valence vibrations of hydroxyl groups in the resulting complex compounds are observed in the 3500–3400 cm^{-1} area, and the valence oscillations of the carboxyl groups in the GA are observed in the field 1725–1690 cm^{-1} (Table 3). In the IR spectrum of the supramolecular complex GA formed with menthol, asymmetric valence oscillations of the -CH_3 group were observed in 2924–2927 cm^{-1}. At the wavelength of 2857–2860 cm^{-1}, it is noted that the symmetric valence oscillations of the -CH_2 group are weak, and in the area 1085 cm^{-1} there are valence oscillations of the -O^- group.

Due to the absence of chromophore groups in the L-(–)- menthol molecule, no apparent absorption was observed in their UV spectra. Therefore, the IR spectra of menthol and its complex with GA were studied.

In the formation of a supramolecular compound, it was found that the host molecule contains several active bonds that form several bonds. It was noted that the host and guest geometric structure, that is, the diameter of the gap in the receptor molecule, corresponds to the radius of the substrate molecule. The complementarity feature allows the host molecule to select guests in a well-defined structure.

It is worth noting that the GA molecule has a "guest-host" formation of clathrate compounds, its complexity with a number of medications used in medicine, to increase their activity and increase the treatment index by the effect of molecular capsules [40–41].

In the picture below, the supramolecular complex of 4:1 GA with mentolol was recorded by using "Shimadzu" IR-Fure spectrophotometer device (Japan) and "Perkin-Elmer Spectrum IR" – 10.6.1 in the absorption range of 3400–3500 cm^{-1} (Figure 3; Figure 4).

In this case, the shape of the oscillation is explained by the amplitude of all the atoms vibrating at the same frequency and, in turn, the change in the length of the chemical bond and the interconnection angle at normal vibrations.

If the angles between atoms change in the course of vibration, this type of oscillation is called deformation vibration. However, pure valence or pure deformation oscillations occur only in linear molecules or in highly symmetric molecules and ions (octahedrons, tetrahedrons, squares, etc.). In most multi-atom molecules and ions, mixed valence-deformation oscillations occur together, and the angles between them change as the valence bond distances change.

One of the most widely used methods for the identification of menthol with GA derived supramolecular compounds has been the use of high-performance liquid chromatography. Chromatography isoconate flow rate 1ml/min and acetylitrile: acetate buffer system was used as an eulent.

The following are the chromatographic conditions:

– chromatograph- Agilent Technologies – 1200
– column – Exlipce XDB – C18, 5mkm, 4.8 × 150 mm
– eluent-acetoneitrile: acetone buffer (21:89)
– detector – UV (254nm)
– regime-isocratic
– Temperature – 25 ˚C
– vcol-5mkl

The results showed that the amount of glycyrrhizic acid in the supramolecular complex compounds was theoretically calculated and the error rate was ± 1–1.5%.

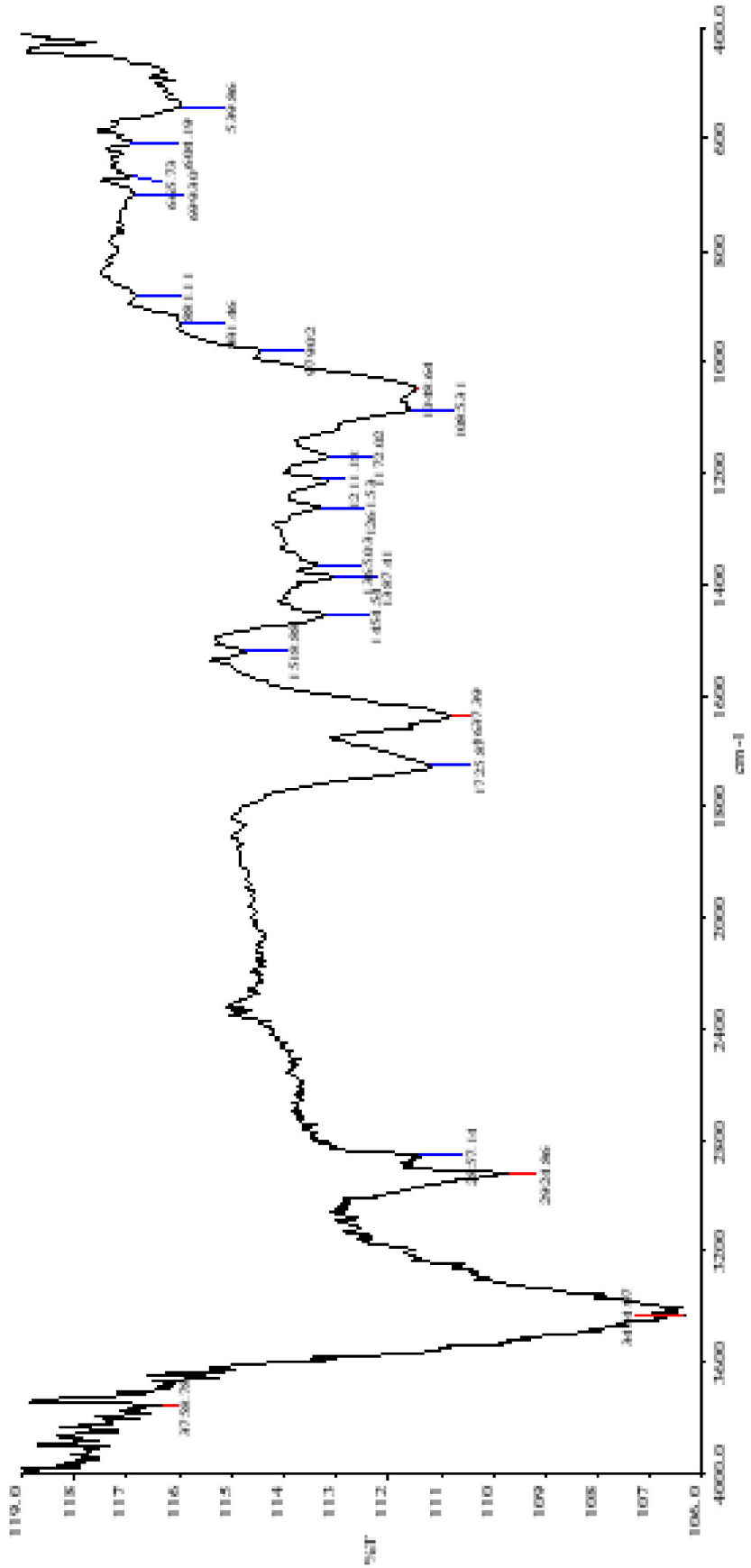

Figure 3. IR-Fure spectra of the supramolecular complex GA generated by menthol. The IR-Fure spectra were recorded using an IR-Fure spectrophotometer device (Perkin-Elmer Spectrum IR – 10.6.1; USA) in the absorption range of 3400–3500 cm^{-1}. The spectra were recorded at a resolution of >4 cm^{-1}. The vacuum conditions (0.1–0.05 mm s.u) were pressed in the form of a spectral pure KBr ("Merck", Germany) for adsorption of moisture in the test samples

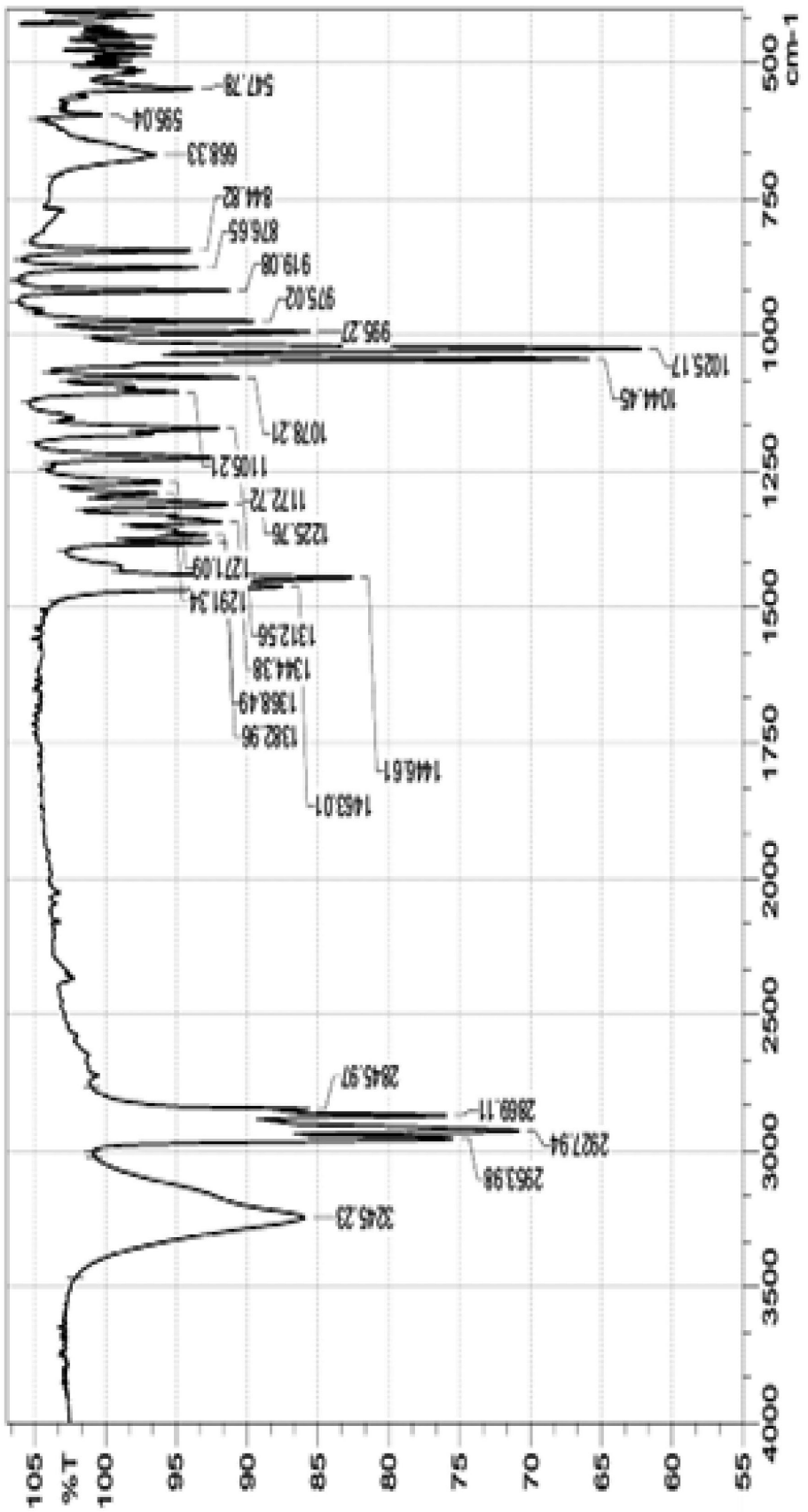

Figure 4. IR spectrum of menthol. The IR-Fure spectra were recorded using an IR-Fure spectrophotometer device (Perkin-Elmer Spectrum IR – 10.6.1; USA) in the absorption range of 3400–3500 cm^{-1}. The spectra were determined at a resolution value of > 4 cm^{-1}. The vacuum conditions (0.1–0.05 mm s.u) were pressed in the form of a spectral pure KBr ("Merck", Germany) for adsorption of moisture in the test samples

Quantitative determination was performed with respect to standard GA solution. Because the menthol molecule does not contain chromophore groups, it cannot be detected by simple spectroscopic methods. Therefore, in our experiments, we used quantitative GA to qualitatively and quantitatively determination. Quantitative computations were compared relative to the peak area at the time of the standard solution retention (Table 4).

Table 4.– Results of the HPLS-based study of supramolecular complex of GA with menthol

Complexes	Time for holding complexes in the column, min.	Quantity calculated from the theoretical point. mg/100ml	Result obtained practically mg/100ml
GA	6.967	100.0	100.0
2:1	7.118	100.0	98.7
4:1	7.129	100.0	99.1
9:1	7.159	100.0	98.6

Initial agents for the IR-Fure spectra GA: Menthol (4:1) supramolecular complex recorded in the experiments by using an IR-Fure spectrophotometer device (Perkin-Elmer Spectrum IR-10.6.1; USA). The correlation coefficients of functional groups in the molecules GA ($C_{42}H_{62}O_{16}$; "Biochemica", Germany)and ISK ($C_{12}H_9NO_2$; Biochemica, Germany) were 0.84 and 0.70, respectively.

It was noted that the resulting GA: Menthol (4:1) supramolecular complex is 99.1%.

As can be seen from the values presented in (Table 2), the quantities of theoretically obtained complexes are consistent with the results obtained in practice, and their difference does not exceed 1.0–1.5%. This proves that the method of HPLS can be used to standardize the obtained supramolecular complex compounds.

Qualitatively standard of GA hold time in the column was set as (6.5–7.0 min).

Chemical synthesis the supramolecular complexes of GA with physiologically active compounds provide lot perspectives to use in agriculture. Our near future work will be addressed to test this newly supramolecular compounds based on GA: Menthol for plant growth and (a) biotic stress resilience.

Conclusion

In the experiments, we have obtained the supramolecular complexes of glycyrrhizic acid and menthol. The resulting supramolecular complexes have the highest yields in the ratio of 4:1, and the resulting GA: Menthol (4:1) complex has been chemically identified by comparing the IR-Fure spectra of the primary agents.

Initial agents of the supramolecular complex GA: Menthol (4:1) (GA ($C_{42}H_{62}O_{16}$; Biochemica, Germany) recorded using an IR-Fure spectrophotometer device (Perkin-Elmer Spectrum IR – 10.6.1; USA).) and the coefficients of functional groups in the molecules consistence of ISK ($C_{12}H_9NO_2$; Biochemica, Germany) were 0.84 and 0.70.

References:

1. Hiroshi F., Katsumi G., Mamoru T. The pharmacological activity of licorice root extracts // Chem. Pharm. Bull.1996. – V. 36(10).– P. 4174–4176.
2. Яковшин Л. А. Молекулярные комплексы тритерпеновых гликозидов с биологически активными веществами: Получение, химико-фармацевтические свойства и биологическая активность // Дисс. на соискание учен. ст. д.хим.н.– Севастополь, 2018.– С. 10–238.
3. Marsh C. A., Lewy G. A. Glucuronide metabolism in plants. 3. Triterpene glucuronides // Journal of Biochemistry.1955.– V. 63(1). – P. 9–14.

4. Сумина Е. Г., Данчук А. И., Угланова В. З., Сорокина О. Н. Сравнительное определение глицирризиновой кислоты методами ТСХ и ВЭЖХ в подвижных фазах, модифицированных пав и органическими растворителями // Бутлеровские сообщения.– Изд-во ООО «Инновационно–изд. дом Бутлеровское наследие» (Казань).2015.– Том. 44.– № 12. – С. 94–100.
5. Корниевская В. С. Изучение супрамолекулярных структур глицирризиновой кислоты в растворах методами ^{1}Н ЯМР и ХПЯ // Автореферат дисс.к.хим.н.– Новосибирск, 2008.– С. 3–20.
6. Половяненко Д. Н. Супрамолекулярные комплексы «гость-хозяин» с участием спиновых ловушек и нитроксильных радикалов // Авторферат дисс.к.физ.-мат.н.– Новосибирск, 2009.– С. 4–19.
7. Борисенко С. Н., Ветрова Е. В., Лекарь А. В., Филонова О. В., Борисенко Н. И. Масс-спектрометрия супрамолекулярных комплексов глицирретиновой кислоты с антибиотиком стрептоцидом // Химия растительного сырья.2015. – № 3. – С. 127–134.
8. Толстикова Т. Г., Толстиков А. Г., Толстиков Г. А. На пути к низкодозным лекарствам // Вестник Российской академии наук.2007.– Т. 77.– № 10. – С. 867–874.
9. Душкин А. В., Метелева Е. С., Чистяченко Ю. С., Халиков С. С. Механохимическое получение и свойства твердых дисперсий, образующих водорастворимые супрамолекулярные системы // Фундаментальные исследования.2013. – № 1–3. – С. 741–749.
10. Groen J., Pelser H., Frenkel M. et al. Effect of glycyrrhizinic acid on the electrolyte metabolism in Addison's disease // Journal of Clinical Investigation.1952. – V.31(l).– P. 87–91.
11. Толстиков Г. А., Муринов Ю. И., Балтина Л. А. и др. Комплексы (3 глицирризиновой кислоты с простагландинами. Новый класс утеротонически активных веществ // Химико-фармацевтический журнал.1991.– Т. 25(3). – С. 42–44.
12. Gusakov V. N., Maistrenko V. N., Saflullin P. P. Thermodynamics of formation of molecular complexes of aromatic nitro derivatives with lincomycin and P-glycyrrhizic acid // Russian Journal of General Chemistry.– 2001.– V.71(8).– P. 1307–1310.
13. Корниевская В. С. Изучение супрамолекулярных структур глицирризиновой кислоты в растворах методами ^{1}Н ЯМР и ХПЯ // Автореферат дисс.к.хим.н.– Новосибирск, 2008.– С. 5–20
14. Борисенко С. Н., Ветрова Е. В., Лекарь А. В., Филонова О. В., Борисенко Н. И. Масс–спектрометрия супрамолекулярных комплексов глицирретиновой кислоты с антибиотиком стрептоцидом // Химия растительного сырья.2015.– № 3.– С. 89–94.
15. Хаитбаев А. Х. Супрамолекулярный комплекс мегосина // Сборник материалов IX Международного симпозиума «Фенольные соединения: фундаментальные и прикладные аспекты».– Москва, 2015.– С. 155–158.
16. Ветрова Е. В., Лекарь А. В., Максименко Е. В., Хизриева С. С., Бугаева А. Ф., Борисенко Н. И. Масс–спектрометрия супрамолекулярных комплексов глицирризиновой кислоты и трептомицина // Химия растительного сырья.2016.– № 3.– С. 27–34.
17. Nurkeeva Z. S., Khutoryanskiy V. V., Mun G. A., Sherbakova M. V., Ivaschenko A. T., Aitkho-zhina N. A. Polycomplexes of poly(acrylic acid) with streptomycin sulfate and their antibacterial activity // European Journal of Pharmaceutics and Biopharmaceutics.2004.– V. 57.– P. 245–249.
18. Wrzesniok D., Beberok A., Otreba M., Buszman E. Effect of streptomycin on melanogenesis and antioxidant status in melanocytes // Mol. Cell Biochem.2013.– V. 383.– P. 77–84.

19. Silva W. F., Cecilio S. G., Magalhaes C. L. B., Ferreira J. M. S, Totola A. H., de Magalhaes J. C. Combination of extracts from Aristolochia. Cymbifera with streptomycin as a potential antibacterial drug // Springer Plus.2013.– V. 2(430).– P. 1–7.
20. Kooti M., Gharineh S., Mehrkhah M., Shaker A., Motamedi H. Preparation and antibacterial activity of $CoFe_2O_4/SiO_2$/Ag composite impregnated with streptomycin // Chemical Engineering Journal. 2015.– V. 259(1). – P. 34–42.
21. Sell CS: A fragrant introduction to terpenoid chemistry. Royal Society of Chemistry, 2003.– P. 76–77.
22. Al-Rawi A and Chakravarty H. L. Medicinal plants of Iraq. Ministry of Agriculture and Irrigation, State Board for Agricultural and Water Resources Research, National Herbarium of Iraq, – Baghdad; 1988.– 65 p.
23. Брежнева Т. А., Мальцева А. А., Боева С. А., Сливкин А. И., Мироненко Н. В. Исследование возможности количественного определения тритерпеновых сапонинов методом УФ-спектрофотометрии // Вестник ВГУ (Серия: Химия. Биология. Фармация).2007.– № 2. – С. 142–143.
24. Мироненко Н. В., Брежнева Т. А., Михина И. А., Селеменев В. Ф. Сравнительный анализ методик количественного определения тритерпеновых сапонинов – производных олеаноловой кислоты // Заводская лаборатория. Диагностика материалов.2009.– Т. 75.– № 5. – С. 19–23.
25. Мироненко Н. В., Брежнева Т. А., Селеменев В. Ф. УФ-спектрофотометрическое определение тритерпеновых сапонинов – производных олеаноловой кислоты // Химия растительного сырья.2011. – № 3. – С. 153–157.
26. Крахмалев И. С., Губанова Л. Б., Хаджиева З. Д. Разработка методик качественного и количественного анализа спрея на основе густых экстрактов эвкалипта прутовидного и солодки голой // Фармацевтические науки. Фундаментальные исследования.2012. – № 5. – С. 431–435.
27. Абжалелов Б. Б. и др. Получение глицирризиновой кислоты из солодкового корня // Международный журнал экспериментального образования.2016.– № 5–1. – С. 100–104.
28. Столярова О. В., Фаррахова Г. Ф., Балтина Л. А., Габбасов Т. М., Баширова Р. М., Кондратенко Р. М., Балтина Л. А. Выделение глицирризиновой кислоты и ее моноаммонийной соли из корней и корневищ солодки коржинского (*Glycyrrhiza korshinskyi* Grig) // Вестник Башкирского университета.2008.– Т. 3.– № 2. – С. 256–258.
29. Гармаева Е. А. Разработка и стандартизация комплексного растительного средства, рекомендуемого для профилактики простатита // Автореферат дисс.к.фарм.н.– Улан-Удэ, 2007.– С. 3–20.
30. Астафьева О. В., Сухенко Л. Т., Егоров М. А. Противомикробная активность выделенных биологически активных веществ и экстракта корня *Glycyrrhiza glabra* L. // Химия растительного сырья. 2013.– № 3.– С. 261–263.
31. Шлотгауэр А. А. Исследование взаимодействия аторвастатина с тритерпеновым гликозидом глицирризиновой кислотой методом ЯМР релаксации в растворах // Фундаментальные исследования. 2013.– № 10–3.– С. 553–556.
32. Mukhopadhyay M., Panja P. A novel process for extraction of natural sweetener from licorice (*Glycyrrhiza glabra*) roots // Separ. Purif. Technol. 2008. - V. 63. – P. 539–545.
33. Рыбальченко А. С., Голицин В. П., Комарова Л. Ф. Исследование экстракции солодкового корня // Химия растительного сырья.2002. – № 4. – С. 55–59.
34. Kim H.-S. et. al. Effects of modifiers on the supercritical CO_2 extraction of glycyrrhizin from licorice and the morphology of licorice tissue after extraction // Biotechnology and Bioprocess Engineering.2004.– V. 9(6). – P. 447–453.

35. Хабибрахманова В. Р. и др. Переработка шрота корня солодки. II. Тритерпеноидные и флавоноидные вещества этанольных экстрактов // Химия растительного сырья.2016. – № 2. – С. 97–102.
36. Гагиева Л. Ч. и др. Определение технологических параметров получения жидкого экстракта из солодки голой // Известия Горского гос. аграрного ун-та. 2011.– Ч. 2.– Т. 48. – С. 266–268.
37. Charpe T. W., Rathod V. K. Extraction of glycyrrhizic acid from licorice root using ultrasound: Process intensification studies // Chemical Engineering and Processing: Process Intensification.2012. – V. 54. – P. 37–41.
38. Тихомирова К. С. и др. Экстракция глицирризиновой кислоты из корня солодки в среде субкритической воды // Сверхкритические флюиды: теория и практика.2008. – № 3. – С. 71–74.
39. Астафьева О. В., Сухенко Л. Т., Егоров М. А. Противомикробная активность выделенных биологически активных веществ и экстракта корня *Glycyrrhiza glabra* L. // Химия растительного сырья.2013.– № 3. – С. 261–263.
40. Далимов Д. Н., Мухамедиев М. Г., Хамидова Г. Р., Гафуров М. Б., Абдуллаев Н. Дж., Левкович М. Г., Юлдашев Х. А., Матчанов А. Д. Физико-химические свойства водных растворов клатратов моноаммониевой соли глицирризиновой кислоты с бензойной и салициловой кислотами. Актуальные проблемы развитие полимерной химии". – Тошкент. 2011.– С. 164–165.
41. Nazarova F. A., Gafurov M. B., Tilyabaev Z., Dalimov D. N. Supremolekular complexes of alkaloids exerting anti-cholinesterase activity.международная научная конференция "Актуальные проблемы развитие биорганической химии".– Ташкент.-15–16 ноября 2013.– С. 45–46.

Section 4. Machinery construction

https://doi.org/10.29013/AJT-20-9.10-23-35

Vasenin Valery Ivanovitch,
associate professor, candidate of technical sciences,
department "Innovation Technologies of Engineering"
State National Research Polytechnical University of Perm,
E-mail: vaseninvaleriy@mail.ru
Bogomjagkov Aleksey Vasilievitch,
senior teacher
Sharov Konstantin Vladimirovich,
senior teacher

STUDY OF THE FILLING OF THE MOULD WITH LIQUID THROUGH A STEP GATE SYSTEM UNDER A FLOODING LEVEL

Abstract. A step gating system has been studied to determine the velocity and flow of liquids in each gate and throughout the system when filling the mould with liquids under a flooding level. Bernoulli's equation was used to calculate such systems with variable fluid flow rate, although it has been derived theoretically and tested practically for a constant fluid flow rate. It calculates the filling of each mould volume between gate. Some of the gates work at a constant head, others at variable head. The resistance coefficients, flow rates of all working gates and the flow rate of liquid from the gates change in accordance with the metal level in the mould. A method for calculating how the mould should be filled with metal under a flooding level has been created. As the level rises in the mould, the flow rate of liquid from the lower gate decreases and from the upper gate increases.

Keywords: pouring basin, sprue, sprue basin, gate, resistance coefficient, flow coefficient, flow velocity, liquid flow rate.

Introduction

In the article [1], an L-shaped gating system (GS) parameters were calculated for the first time with the determination of the resistance coefficient and flow rate of each gate, the fluid velocity in each gate and the flow rate throughout the system. Then the branched [2], cross-shaped [3], P-shaped [4], single- and double-ring systems [5; 6], L-shaped system with a variable cross-section sprue basin [7; 8], and a system with two sprues of the same and different height [9; 10] were theoretically and experimentally investigated. Vertical GS systems with different number of gates on steps were studied [11; 12]. A vertical two-ringed GS was studied [13], as well as the joint operation of a horizontal ring system with a step [14] and a branched system [15]. Bernoulli's equation was used in the calculations of multi gated GSs, although it is derived for a constant flow (mass) [16, P. 10; 17,

P. 205], i.e. for single gate GS. Consequently, BE also works with variable flow rate, although it is not clear why it works. And the possibility of using the BE in the calculation of GS parameters with variable flow rates from maximum to zero in the sprue basin (runner) has not been theoretically proved. However, none of these GSs have been studied when filling the mould with liquid metal under a flooding level – this is the second stage of filling the mould. In the first stage, the liquid metal is drained from the top down from the gates to the mould. Therefore, it seems expedient to investigate such a complex GS as a step gating system, where gates are located at different levels (steps) and the filling of the mould goes under a flooding level with the gate slots being sequentially covered by the rising liquid.

Research methods

The step gating system is shown in (Figure 1). The system consists of a mould, sprue, horizontal sprue basin, vertical sprue basin and 4 identical I–IV gates. The inner diameter of the mould is 272 mm and the height of the water in the mould is 103.5 mm. The liquid level H – the vertical distance from the section 1–1 in the mould to the longitudinal axis of the horizontal basin (0–0 plane of reference) – was maintained constant by continuous refilling of water into the mould and draining the excess through a special slot in the mould: $H = 0.6135$ m. The size of the mould in the horizontal cross-section is 252 × 253 mm.

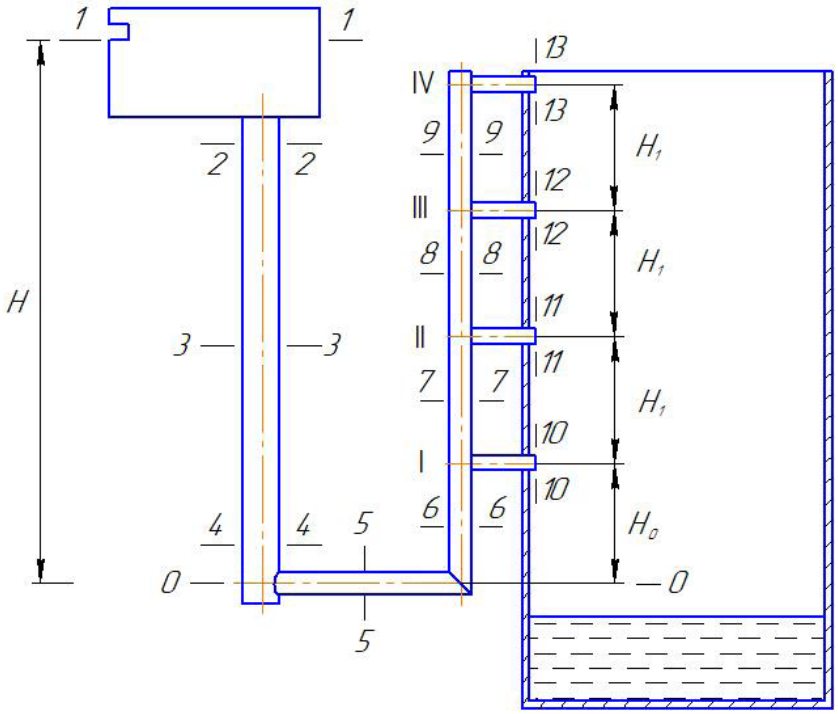

Figure 1. Gating system for filling the mould with liquid under a flooding level

Main body

First we calculate the liquid flow rate from only one gate I from above into the mould, not under a flooding level. We will make up a BE for sections 1–1 and 10–10 of GS:

$$H = H_0 + \alpha \frac{v_{10}^2}{2g} + h_{1-10}, \qquad (1)$$

where H_0 – is the vertical distance from the 0–0 reference plane to the horizontal axis of the gate I, m; $H_0 = 0.124$ m; α – is the irregularity ratio of the velocity distribution over the flow cross section (Coriolis coefficient); let us assume $\alpha = 1.1$ [17, P. 108]; v_{10} – is the metal velocity in the cross section 10–10 of gate I, m/s; g – is the gravity acceleration; $g = 9.81$ m/s^2; h_{1-10} – is the head losses in the flow

of liquid from the cross section 1–1 to the cross section 10–10, m. These head losses

$$h_{1-10} = \left(\zeta_{sp} + \lambda\frac{l_{sp}}{d_{sp}}\right)\alpha\frac{v_{sp}^2}{2g} + \left(\zeta_{sb} + \lambda\frac{l_{sp-I}}{d_{sb}} + \zeta\right)\alpha\frac{v_5^2}{2g} + \left(\zeta_g + \lambda\frac{l_g}{d_g}\right)\alpha\frac{v_{10}^2}{2g}, \quad (2)$$

where ζ_{sp}, ζ_{sb}, ζ, ζ_g are local resistance coefficients of metal entrance from the mould to the sprue, turn from the sprue to the horizontal sprue basin, turn from the section 5–5 of the horizontal sprue basin to the section 6–6 of the vertical sprue basin, turn from the section 6–6 of the vertical sprue basin to the gate I with an output section 10–10; λ – is the friction loss coefficient; l_{sp} – is the length (height) of the sprue, m; $l_{sp} = 0.518$ m; d_{sp}, d_{sb}, d_g hydraulic diameters of the sprue, sprue basin and gate I, m; $d_{sp} = 0.02408$ m, $d_{sb} = d_5 = d_6 = d_7 = d_8 = d_9 = 0.01603$ m, $d_g = 0.00903$ m; v_{sp} – is the fluid velocity in the sprue, m/s; v_5 – fluid velocity in the section 5–5 of the sprue basin, m/s; l_{sp-I} – is the distance from the sprue to the gate I, m; $l_{sp-I} = 0.249$ m; l_g gate length, m; $l_g = 0.0495$ m. Flow rate in GS when pouring from the top is determined by the metal velocity v_{10} n the output section 10–10 of the gate I and its cross-sectional area: $Q = v_{10}S_g$ The remaining fluid velocities in GS channels are determined by the flow continuity equation:

$$Q = v_{sp}S_{sp} = v_5S_{sb} = v_6S_{sb} = v_{10}S_g, \quad (3)$$

where S_{sp} and S_g are the cross-section areas of the sprue and sprue basin, m^2.

$S_{sb} = S_5 = S_6 = S_7 = S_8 = S_9$, $v_5 = v_6$. Let us express all metal velocities in (2) in terms of the velocity v_{10}, using the flow continuity equation (3):

$$h_{1-10(10)} = \alpha\frac{v_{10}^2}{2g}\left[\left(\zeta_{sp} + \lambda\frac{l_{sp}}{d_{sp}}\right)\left(\frac{S_g}{S_{sp}}\right)^2 + \left(\zeta_{sb} + \lambda\frac{l_{sp-I}}{d_{sb}} + \zeta\right)\left(\frac{S_g}{S_{sb}}\right)^2 + \zeta_g + \lambda\frac{l_g}{d_g}\right]. \quad (4)$$

Let us denote the expression in square brackets as $\zeta_{1-10(10)}$: the resistance coefficient of the system from section 1–1 to section 10–10, reduced to the fluid velocity in section 10–10,

$$\zeta_{1-10(10)} = \left(\zeta_{cm} + \lambda\frac{l_{cm}}{d_{cm}}\right)\left(\frac{S_n}{S_{cm}}\right)^2 + \left(\zeta_\kappa + \lambda\frac{l_{cm-I}}{d_\kappa} + \zeta\right)\left(\frac{S_n}{S_\kappa}\right)^2 + \zeta_n + \lambda\frac{l_n}{d_n}. \quad (5)$$

Now (1) can be written as: $H - h_0 = \alpha v_{10}^2(1 + \zeta_{1-10(10)})/2g$. And system flow rate from section 1–1 to section 10–10, reduced to velocity v_{10},

$$\mu_{1-10(10)} = \left(1 + \zeta_{1-10(10)}\right)^{-1/2}. \quad (6)$$

Velocity

$$v_{10} = \mu_{1-10(10)}\sqrt{2g\left(H - H_0\right)/\alpha}. \quad (7)$$

We find the flow rate Q using (3). Let us assume, as in works [18; 19], that the friction loss coefficient is $\lambda = 0.03$. The local resistance coefficient of the entry from the mould to the sprue, depending on the radius of rounding of the entrance edge, is determined by [20, P. 126]: $\zeta_{sp} = 0.12$. Local resistance coefficients [21]: $\zeta_{sb} = 0.396$, $\zeta = 0.885$, $\zeta_g = 0.334$.

Results of (5)–(7) and (3) ratio calculations: $\zeta_{1-10(10)} = 0.689505$, $\mu_{1-10(10)} = 0.769343$, $v_{10} = 2.273264$ m/s, $Q_{10} = 145.584510 \cdot 10^{-6}$ m^3/s.

Volume of mould between 0–0 axis and longitudinal axis of gate I $W_{0-I} = 0.252 \cdot 0.253 \cdot 0.124 = 7905.744 \cdot 10^{-6}$ m^3. Time required to fill this volume by gate I $t = W_{0\_I}/Q_{10} = 54.303$ s.

Distance between gates I and II, II and III, III and IV $H_1 = 0.119$ m, and volume of the mould between gates $W = 0.252 \cdot 0.253 \cdot 0.119 = 7586.964 \cdot 10^{-6}$ м^3.

When filling the mould under the flooding level, BE for sections 1–1 and *X*–*X*, it will be written down as follows [17, P. 229; 22, P. 227]:

$$H = H_0 + H_{1-X} + h_{1-10} + h_{1-X} + \alpha\frac{v_m^2}{2g}, \quad (8)$$

where H_{1-X} is the vertical distance from the horizontal axis of gate I to section *X*–*X* above gate I, m; h_{I-X}

head loss during fluid movement from gate I to section X–X in mould, m. These head losses $h_{1-X} = \lambda \frac{H_{1-X}}{d_m} \alpha \frac{v_m^2}{2g}$, where d_m is the hydraulic diameter of the mould, m; v_m is the fluid velocity in the mould, m/s. Fluid velocity in the mould: $v_m \approx 0$. The velocity head of the liquid in the mould $\alpha v_m^2 / 2g$ and he head loss in the mould h_{I-X} and therefore be ignored. Mould head loss when filling the mould under level by gate I

$$h_{1-10} = \left(\zeta_{sp} + \lambda \frac{l_{sp}}{d_{sp}} \right) \alpha \frac{v_{sp}^2}{2g} + \left(\zeta_{\kappa} + \lambda \frac{l_{sp-I}}{d_{sb}} + \zeta \right) \alpha \frac{v_5^2}{2g} + \left(\zeta_g + \lambda \frac{l_g}{d_g} \right) \alpha \frac{v_{10}^2}{2g} + \zeta_{out} \alpha \frac{v_{10}^2}{2g}, \quad (9)$$

where ζ_{out} is the local resistance coefficient for the output of liquid from gate I to the mould (large vessel): $\zeta_{out} = 1$ [17, P. 187]. This means that all the velocity head in gate I equal to $\alpha v_{10}^2 / 2g$, is lost when the liquid leaves the gate for a large vessel, and the liquid level rise rate in the mould is ≈ 0.

Resistance coefficient

$$\zeta_{1-10(10)} = \left(\zeta_{sp} + \lambda \frac{l_{sp}}{d_{sp}} \right) \left(\frac{S_g}{S_{sp}} \right)^2 + \left(\zeta_{sb} + \lambda \frac{l_{sp-I}}{d_{sb}} + \zeta \right) \left(\frac{S_g}{S_{sb}} \right)^2 + \zeta_g + \lambda \frac{l_g}{d_g} + \zeta_{out}. \quad (10)$$

The formula (8) will be as follows:

$$H - H_0 - H_{1-X} = h_{1-10(10)} = \zeta_{1-10(10)} \alpha v_{10}^2 / 2g. \quad (11)$$

That is to say, for the flow for level difference, the difference between the steps is equal to the head loss. When flowing from above, the level difference is equal to the head velocity and head loss, as seen in (1)

Flow coefficient

$$\mu_{1-10(10)} = \left(\zeta_{1-10(10)} \right)^{-1/2}. \quad (12)$$

Liquid velocity in gate I when only this gate is operating

$$v_{10} = \mu_{1-10(10)} \sqrt{2g(H - H_0 - H_{I-X}) / \alpha}. \quad (13)$$

When filling under the level, the resistance coefficient of (10) increased by $\zeta_{out} = 1$, and (12) compared to (6) eliminated 11. This means that the flow rate $\mu_{1-10(10)}$ when the liquid is poured from top to bottom from the gate to the mould for filling under a flooding level.

When filling under a flooded level (above the horizontal axis of gate I) above gate I, the level of liquid in the mould increases all the time, and the system head decreases from $H - H_0$ to a minimum when the liquid level reaches the horizontal axis of gate IV – $H - H_0 - 3H_1$. As is already known (see e.g. [23]), in this case the rated head is calculated by the following:

$$\sqrt{H_{rt}} = \frac{\sqrt{H - H_0} + \sqrt{H - H_0 - 3H_1}}{2}. \quad (14)$$

This is the exact formula for determining the rated head when filling out a mould with a constant section in height. And formula (13) should be as follows:

$$v_{10} = \mu_{1-10(10)} \sqrt{2g / \alpha} \sqrt{H_{rt}}. \quad (15)$$

Using (14) $\sqrt{H_{rt}} = 0.531834$ m$^{1/2}$, and the time of filling in the top part of the mould of height $3H_1$ equals 205.675 s. The total time of filling the mould with liquid from gate I is 259.979 s.

We calculate the flow of liquid from gates II, III or IV in the same way, with the following corrections. When gate II operates in formula (7), instead of "$H - H_0$" it should be "$H - H_0 - H_1$", for gate III – "$H - H_0 - 2H_1$", for gate IV – "$H - H_0 - 3H_1$". For gate II in (5), we should use $l_{sp-I} = H_1$, instead of l_{sp-I}, for gate III – we should use $l_{sp-I} + 2H_1$ instead, fore IV – $l_{sp-I} + 3H_1$.

The results of the calculations are given in (Table 1).

Let us calculate filling a part of the mould with height of H_0 when gates I and II are operating. BE for sections 1–1 mould and 10–10 of gate I:

$$H = H_0 + \left(\zeta_{sp} + \lambda \frac{l_{sp}}{d_{sp}} \right) \alpha \frac{v_{sp}^2}{2g} + \left(\zeta_{\kappa} + \lambda \frac{l_{sp-I}}{d_{sb}} + \zeta \right) \alpha \frac{v_5^2}{2g} + \left(\zeta_{10} + \lambda \frac{l_g}{d_g} \right) \alpha \frac{v_{10}^2}{2g}. \quad (16)$$

BE for sections 1–1 mould and 11–11 of gate II:

Table 1.– Parameters of the gating system with one working gate

Operating gate, filling volume	Parameters		
	$\sqrt{H_{rt}}$, m$^{1/2}$	v, m/s	τ, s
I			
0 – I	0.700	2.273	54.303
I – II	0.654	2.125	55.737
II – III	0.555	1.804	65.685
III–IV	0.433	1.406	84.254
0 – IV			259.979
II			
0 – I	0.609	1.965	62.831
I – II	0.609	1.965	60.297
II – III	0.555	1.792	66.119
III–IV	0.433	1.397	84.811
0 – IV			274.058
III			
0 – I	0.501	1.608	76.758
I – II	0.501	1.608	73.663
II – III	0.501	1.608	73.663
III–IV	0.433	1.388	85.365
0 – IV			309.449
IV			
0 – I	0.364	1.160	106.433
I – II	0.364	1.160	102.141
II – III	0.364	1.160	102.141
III–IV	0.364	1.160	102.141
0 – IV			412.856

$$H = H_0 + H_1 + \left(\zeta_{sp} + \lambda\frac{l_{sp}}{d_{sp}}\right)\alpha\frac{v_{sp}^2}{2g} + \left(\zeta_{sb} + \lambda\frac{l_{sp-I}}{d_{sb}} + \zeta\right)\alpha\frac{v_5^2}{2g} + \left(\zeta_7 + \lambda\frac{H_1}{d_{sb}}\right)\alpha\frac{v_7^2}{2g} + \left(\zeta_g + \lambda\frac{l_g}{d_g}\right)\alpha\frac{v_{11}^2}{2g}. \quad (17)$$

$\mu_{1-10(10)} = 0.769$, $\mu_{1-11(11)} = 0.764$, $\mu_{1-12(12)} = 0.759$, $\mu_{1-13(13)} = 0.754$

Where v_7 is the metal velocity in section 7–7, m/s. In (16) and (17) ζ_{10} is the resistance coefficient for a branch of a flow part from section 6–6 of the sprue basin to gate I with output section 10–10; ζ_7 is the resistance coefficient for a passage in the sprue basin from section 6–6 to section 7–7 with a branch of a flow part to gate I The resistance coefficients caused by the branching of a part of the flow from the sprue basin to the gate will be calculated using formulas for T-shapes [16, p. 112–115]. Resistance coefficient for the passage in the sprue basin at branching part of a flow into the gate

$$\zeta_{ps} = 0.4\left(1 - v_{ps}/v_{sb}\right)^2 / \left(v_{ps}/v_{sb}\right)^2, \quad (18)$$

and the resistance coefficient to a branch of the flow to the gate

$$\zeta_{br} = \left[1 + \tau\left(v_g/v_{sb}\right)^2\right] / \left(v_g/v_{sb}\right)^2, \quad (19)$$

where v_{sb} and v_{ps} the metal velocity in the sprue basin before and after flow branching into the gate, m/s; v_g is the liquid velocity in the gate, m/s; τ is the ratio. For our case $S_g / S_{sb} = 0.317$ $\tau = 0.15$ [24]. Ratio ζ_{ps} is calculated as reduced to the flow velocity v_{ps}, and ζ_{br} the velocity in the gate v_g. As evident, ζ_{ps} and ζ_{br} are dependent on velocity ratios v_{ps} / v_{sb} and v_g / v_{sb}, specifically, on v_7 / v_6 and v_{10} / v_6, which are unknown.

Let us introduce the following notation: $x = v_{11} / v_{10}$, $w = v_7 / v_6$. Then $v_{11} = xv_{10}$, a $v_{10} = v_{11} / x$. Liquid flow rate in the system $Q = v_{sp}S_{sp} = = (v_{10} + v_{11})S_g = (v_{10} + xv_{10})S_g = v_{10}(1+x)S_g = v_{10}S_{ps(10)}$, where $S_{ps(10)} = (1+x)S_g$ is the area of gates reduced to velocity v_{10} (taking into account the operation of both gates). Likewise: $Q = (v_{10} + v_{11})S_g = (v_{11} / x + + v_{11})S_g = v_{11}(1/x+1)S_g = v_{11}S_{ps(11)}$, where $S_{ps(11)} = = (1/x+1)S_g$ is the area of gates reduced to velocity v_{11}. $Q = Q_{sp} = Q_5 = Q_6$. And $v_{sp} = v_{10}S_{ps(10)} / S_{sp} = = v_{11}S_{ps(11)} / S_{sp}$, $v_5 = v_6 = v_{10}S_{ps(10)} / S_{sb} = v_{11}S_{ps(11)} / S_{sb}$. $v_7 = v_{11}S_g / S_{sb}$. $w = v_8 / v_7 = v_{11} / (v_{10} + v_{11}) = = v_{11} / (v_{10} + v_{11}) = v_{11} / (v_{11} / x + v_{11}) = 1 / (1/x+1)$.

Let us start calculation with $x = v_{11} / v_{10} = 1$. Where $w = 0.5$, $\zeta_8 = 0.4$, $\zeta_{10} = 0.552788$, cm. formulas (18) and (19). Results: $\zeta_{1-10(10)} = 1.481452$, $\mu_{1-10(10)} = 0.634815$, $v_{10} = 1.875757$ m/s, $\zeta_{1-11(11)} = = 1.325369$, $\mu_{1-11(11)} = 0.655774$, $v_{11} = 1.685782$ m/s, $x = v_{11} / v_{10} = 0.898721$. Let us set $x = 0.898721$, repeat the calculation with the following result $x = 0.878366$. By making similar approximations, we find that $x = 0.8730877$ by calculation – $x = 0.8730876$, and $w = v_7 / v_6 = 0.533878$. We can end calculating x with this, because the difference between the given value and the resulting value is 10^{-7}. The volume of H_0 height is filled by the gates I and II in 34.899 s.

When filling the volume with height H_1 between gates I and II, the liquid is poured out of gate II at constant head $H - H_0 - H_1$, in gate I the head decreases from $H - H_0$ to $H - H_0 - H_1$, and rated head $\sqrt{H_{rt}} = \dfrac{\sqrt{H - H_0} + \sqrt{H - H_0 - H_1}}{2} = 0.639511$ m$^{1/2}$.

We find the liquid velocity in gate I by formula (15) and in gate II by the following formula: $v_{11} = \mu_{1-11(11)}\sqrt{2g(H - H_0 - H_1)/\alpha}$. Let us introduce the following notation: $x = v_{11} / v_{10}$. To start the calculation, we take already calculated value $x = 0.8730877$ and as a result we calculate that $x = 0.908406$. By means of consecutive approximations we find that $x = 0.934463$. The time of filling the volume with height H_1 between gates I and II by those gates is 34.385 s.

The filling of the volume with height $2H_1$ of the gate II to the gate IV occurs at head that is reduced from $H - H_0 - H_1$ to $H - H_0 - 3H_1$. The rated head in this case for gates I and II is $\sqrt{H_{rt}} = 0.486346$ m$^{1/2}$. Let us set $x = 0.934463$, and the result is $x = 1.057637$. The filling time for the mould of $2H_1$ height is 89.523 s. The total filling time for the mould from gates I and II is 158.807 s.

Likewise, we calculate the filling of the mould with liquid from gates I and III, I and IV. The results are in (Tables 2–4).

Let us calculate the filling of the mould with metal from gates I – III. When filling the cavity of the mould with height H_0 the BE for gate I is already found it is (16). For gate II in the formula (17) ζ_g should be replaced by ζ_{11} is the resistance coefficient on the branch of a part of the flow from the section 7–7 of the sprue basin to gate II with the output section 11–11; it is calculated by dependence (19). BE for gate III

$$H = H_0 + 2H_1 + \left(\zeta_{sp} + \lambda\frac{l_{sp}}{d_{sp}}\right)\alpha\frac{v_{sp}^2}{2g} + + \left(\zeta_{sb} + \lambda\frac{l_{sp-I}}{d_{sb}} + \zeta\right)\alpha\frac{v_5^2}{2g} + \left(\zeta_7 + \lambda\frac{H_1}{d_{sb}}\right)\alpha\frac{v_7^2}{2g} + + \left(\zeta_8 + \lambda\frac{H_1}{d_{sb}}\right)\alpha\frac{v_8^2}{2g} + \left(\zeta_g + \lambda\frac{l_g}{d_g}\right)\alpha\frac{v_{12}^2}{2g}, \quad (20)$$

where v_8 is the metal velocity in the section 8–8, m/s; ζ_8 is the esistance coefficient per passage in the sprue basin from section 7–7 to section 8–8 when part of the flow is branched off to gate II; calculated by the formula (19).

Table 2. – Specifications of the gating system with gates I and II

Parameters	Sections filled			
	0–I	I–II	II–III	III–IV
$\zeta_{1-10(10)}$	1.448	1.406	1.549	1.549
$\mu_{1-10(10)}$	0.639	0.645	0.626	0.626
v_{10}, m/s	1.888	1.781	1.468	1.145
$\zeta_{1-11(11)}$	1.431	1.388	1.280	1.280
$\mu_{1-11(11)}$	0.641	0.647	0.662	0.662
v_{11}, m/s	1.649	1.664	1.552	1.210
Q, см^3/с	226.53	217.93	193.46	150.82
v_{11} / v_{10}	0.873	0.934	1.057	1.057
τ, s	34.899	34.385	39.218	50.305

Mould filling time – 158.807 s

Table 3. – Specifications of the gating system with gates I and III

Parameters	Sections filled			
	0–I	I–II	II–III	III–IV
$\zeta_{1-10(10)}$	1.049	1.121	1.765	1.539
$\mu_{1-10(10)}$	0.699	0.687	0.601	0.628
v_{10}, m/s	2.064	1.897	1.410	1.147
$\zeta_{1-12(12)}$	2.057	1.837	1.765	1.309
$\mu_{1-12(12)}$	0.572	0.594	0.601	0.658
v_{12}, m/s	1.211	1.257	1.410	1.203
Q, cm^3/s	209.77	202.01	193.46	150.48
v_{12} / v_{10}	0.587	0.663	1.230	1.049
τ, s	37.688	34.385	37.684	50.417

Mould filling time – 160.174 s

Table 4. – Specifications of the gating system with gates I and IV

Parameters	Sections filled			
	0–I	I–II	II–III	III–IV
$\zeta_{1-10(10)}$	0.798	1.117	1.751	1.528
$\mu_{1-10(10)}$	0.746	0.687	0.603	0.629
v_{10}, m/s	2.203	1.899	1.413	1.149
$\zeta_{1-13(13)}$	4.878	1.871	1.226	1.338
$\mu_{1-13(13)}$	0.412	0.590	0.670	0.654
v_{13}, m/s	0.634	1.250	1.723	1.195
Q, cm^3/s	181.72	201.66	200.86	150.15
v_{13} / v_{10}	0.288	0.658	1.219	1.040
τ, s	43.505	37.622	37.772	50.528

Mould filling time – 169.427 s

Let us use following denotations: $x_1 = v_{11} / v_{10}$, $x_2 = v_{12} / v_{10}$, $w_1 = v_7 / v_6$, $w_2 = v_8 / v_7$. Then $v_{11} = x_1 v_{10}$, $v_{10} = v_{11} / x_1$, $v_{12} = x_2 v_{10}$, $v_{10} = v_{12} / x_2$. Liquid flow rate in the system: $Q = (v_{10} + v_{11} + v_{12}) S_n = (v_{10} + x_1 v_{10} + x_2 v_{10}) S_g = v_{10}(1 + x_1 + x_2) S_g = v_{10} S_{ps(10)}$, where $S_{ps(10)} = (1 + x_1 + x_2) S_g$ – reduced to velocity v_{10} of gate area. Let us denote the following: $Q = (v_{10} + v_{11} + v_{12}) S_n = (v_{11} / x_1 + v_{11} + v_{11} x_2 / x_1) S_g = v_{11}(1 + x_1 + x_2) / x_1 S_g = v_{11} S_{ps(11)}$, where $S_{ps(11)} = (1 + x_1 + x_2) / x_1 S_g$ – reduced to velocity v_{11} of gate area. Similarly: $Q = v_{12}(1 + x_1 + x_2) / x_2 S_g = v_{12} S_{ps(12)}$, where $S_{ps(12)} = (1 + x_1 + x_2) / x_2 S_g$ – reduced to velocity v_{12} of gate area.

$Q = Q_{sp} = Q_5 = Q_6$. and $v_{sp} = v_{10} S_{ps(10)} / S_{sp} = v_{11} S_{ps(11)} / S_{sp} = v_{12} S_{ps(12)} / S_{sp}$. $v_5 = v_6 = v_{10} S_{ps(10)} / S_{sb} = v_{11} S_{ps(11)} / S_{sb} = v_{12} S_{ps(12)} / S_{sb}$.

Velocity v_7 expressed through v_{11} and v_{12} is as follows:

$$v_7 = (v_{11} + v_{12}) S_g / S_{sb} = (v_{11} + x_2 / x_1 v_{11}) S_g / S_{sb} = (x_1 + x_2) / x_1 v_{11} S_g / S_{sb},$$

$$v_7 = (v_{11} + v_{12}) S_g / S_{sb} = (x_1 / x_2 v_{12} + v_{12}) S_g / S_{sb} = (x_1 + x_2) / x_2 v_{12} S_g / S_{sb}.$$

Velocity at sprue basin $v_8 = v_{12} S_g / S_{sb}$.

We also denote the following velocity ratios:

$$w_1 = v_7 / v_6 = (v_{11} + v_{12}) / (v_{10} + v_{11} + v_{12}) = (x_1 v_{10} + x_2 v_{10}) / (v_{10} + x_1 v_{10} + x_2 v_{10}) = (x_1 + x_2) / (1 + x_1 + x_2),$$

$$v_{10} S_g / v_6 S_{sb} = v_{10} S_g / (v_{10} + v_{11} + v_{12}) S_g = v_{10} / (v_{10} + x_1 v_{10} + x_2 v_{10}) = 1 / (1 + x_1 + x_2),$$

$$v_{10} / v_6 = S_{sb} / S_g / (1 + x_1 + x_2),$$

$w_2 = v_8 / v_7 = v_{12} / (v_{11} + v_{12}) = x_2 v_{10} / (x_1 v_{10} + x_2 v_{10}) = x_2 / (x_1 + x_2)$, $v_{11} S_g / v_7 S_{sb} = v_{11} S_g / (v_{11} + v_{12}) S_g = x_1 v_{10} / (x_1 v_{10} + x_2 v_{10}) = x_1 / (x_1 + x_2)$, $v_{11} / v_7 = S_{sb} / S_g x_1 / (x_1 + x_2)$.

All velocity ratios in (16), (17) and (20) are known. Let us introduce the following notation $x_1 = x_2 = 1$, where $w_1 = w_2 = 0.5$, $\zeta_7 = \zeta_8 = 0.4$, $\zeta_{10} = \zeta_{11} = 0.552788$, see (18) and (19). Results: $\mu_{1-10(10)} = 0.5395421$, $v_{10} = 1.593887$ m/s, $\mu_{1-11(11)} = 0.520753$, $v_{11} = 1.338687$ m/s, $\mu_{1-12(12)} = 0.532137$, $v_{12} = 1.127056$ m/s, $x_1 = v_{11} / v_{10} = 0.839888$, $x_2 = v_{12} / v_{10} = 0.707111$. Let use denote $x_1 = 0.839888$, $x_2 = 0.707111$ and recalculate. Through consecutive approximations, we determine that $x_1 = 0.828625$, $x_2 = 0.479566$, and the time to fill a part of the mould with the height H_0 by the gates is 30.657 s.

The filling of the volume H_1 between gates I and II takes place with variable head from gate I and constant head from gates II and III. The volume between Gates II and III is filled at variable head from gate I and II and constant head from gate III. When filling the volume between gates III and IV, the work of gates I to III is carried out at varying head pressures. The results are shown in Table 5. When filling the volume between gates I and II $x_1 = 0.957, x_2 = 0.582$, between gates II and III – $x_1 = 1.136$, $x_2 = 0.935$, between gates III and IV – $x_1 = 1.146$, $x_2 = 1.211$.

Table 5. – Specifications of the gating system with gates I – III

Parameters	Sections filled			
	0–I	I–II	II–III	III–IV
1	*2*	*3*	*4*	*6*
$\zeta_{1-10(10)}$	1.869	2.195	3.065	3.602
$\mu_{1-10(10)}$	0.590	0.559	0.496	0.466
v_{10}, m/s	1.745	1.546	1.163	0.852
$\zeta_{1-11(11)}$	2.162	2.023	2.151	2.507
$\mu_{1-11(11)}$	0.562	0.575	0.563	0.534
v_{11}, m/s	1.446	1.478	1.321	0.976

1	*2*	*3*	*4*	*6*
$\zeta_{1-12(12)}$	5.409	4.535	2.799	2.137
$\mu_{1-12(12)}$	0.395	0.425	0.513	0.565
v_{12}, m/s	0.837	0.800	1.087	1.032
Q, cm^3/s	257.88	251.32	228.64	183.15
v_{11} / v_{10}	0.829	0.957	1.136	1.146
v_{12} / v_{10}	0.480	0.582	0.935	1.211
τ, s	30.657	30.189	33.183	41.424

Mould filling time – 135.453 s

Let us review the filling of the mould with metal when gatesI–IV are operating. BE for gates I and II are already formulated in (16) and (17). For gate III in (20) ζ_g should be replaced by resistance coefficient on the branch of a part of the flow from the section 8–8 sprue basin to gate III with output section 12–12; it is calculated using (19). BE for gate IV is as follows:

$$H = H_0 + 3H_1 + \left(\zeta_{sp} + \lambda\frac{l_{sp}}{d_{sp}}\right)\alpha\frac{v_{sp}^2}{2g} + \left(\zeta_{sb} + \lambda\frac{l_{sp-I}}{d_{sb}} + \zeta\right)\alpha\frac{v_5^2}{2g} + \left(\zeta_7 + \lambda\frac{H_1}{d_{sb}}\right)\alpha\frac{v_7^2}{2g} + \left(\zeta_8 + \lambda\frac{H_1}{d_{sb}}\right)\alpha\frac{v_8^2}{2g} + \left(\zeta_9 + \lambda\frac{H_1}{d_{sb}}\right)\alpha\frac{v_9^2}{2g} + \left(\zeta_g + \lambda\frac{l_g}{d_g}\right)\alpha\frac{v_{13}^2}{2g}, \quad (21)$$

where v_9 is the metal velocity in section 9–9, m/s; ζ_9 – resistance coefficient per passage in the sprue basin from section 8–8 to section 9–9 at branching part of the flow to gate III; calculated as (18).

Let us introduce the following notation: $x_1 = v_{11} / v_{10}$, $x_2 = v_{12} / v_{10}$, $x_3 = v_{13} / v_{10}$, $w_1 = v_7 / v_6$, $w_2 = v_8 / v_7$, $w_3 = v_9 / v_9$. Then $v_{11} = x_1 v_{10}$, $v_{10} = v_{11} / x_1$, $v_{12} = x_2 v_{10}$, $v_{10} = v_{12} / x_2$, $v_{13} = x_3 v_{10}$, $v_{10} = v_{13} / x_3$. Liquidflowrateinthesystem$Q = (v_{10} + v_{11} + v_{12} + v_{13})S_g = (v_{10} + x_1 v_{10} + x_2 v_{10} + x_3 v_{10})S_g = v_{10}(1 + x_1 + x_2 + x_3)S_g = v_{10}S_{ps(10)}$, where $S_{ps(10)} = (1 + x_1 + x_2 + x_3)S_g$ – reduced to velocity v_{10} of gate area. Other areas are as follows: $S_{ps(11)} = (1 + x_1 + x_2 + x_3) / x_1 S_g$, $S_{ps(12)} = (1 + x_1 + x_2 + x_3) / x_2 S_g$, $S_{ps(13)} = (1 + x_1 + x_2 + x_3) / x_3 S_g$.

$Q = Q_{sp} = Q_5 = Q_6$. and $v_{sp} = v_{10}S_{ps(10)} / S_{sp} = v_{11}S_{ps(11)} / S_{sp} = v_{12}S_{ps(12)} / S_{sp} = v_{13}S_{ps(13)} / S_{sp}$, $v_5 = v_6 = v_{10}S_{ps(10)} / S_{sb} = v_{11}S_{ps(11)} / S_{sb} = v_{12}S_{ps(12)} / S_{sb} = v_{13}S_{ps(13)} / S_{sb}$.

Velocity v_7 expressed through v_{11}, v_{12} and v_{13} is as follows:

$v_7 = (v_{11} + v_{12} + v_{13})S_g / S_{sb} = (v_{11} + x_2 / x_1 v_{11} + x_3 / x_1 v_{11})S_g / S_{sb} = (x_1 + x_2 + x_3) / x_1 v_{11} S_g / S_{sb}$,

$v_7 = (v_{11} + v_{12} + v_{13})S_g / S_{sb} = (x_1 / x_2 v_{12} + v_{12} + x_3 / x_2 v_{12})S_g / S_{sb} = (x_1 + x_2 + x_3) / x_2 v_{12} S_g / S_{sb}$,

$v_7 = (v_{11} + v_{12} + v_{13})S_g / S_{sb} = (x_1 / x_3 v_{13} + x_2 / x_3 v_{13} + v_{13})S_g / S_{sb} = (x_1 + x_2 + x_3) / x_3 v_{13} S_g / S_{sb}$.

Velocity v_8 expressed through v_{12} and v_{13} is as follows:

$v_8 = (v_{12} + v_{13})S_g / S_{sb} = (v_{12} + x_3 / x_2 v_{12})S_g / S_{sb} = (x_2 + x_3) / x_2 v_{12} S_g / S_{sb}$,

$v_8 = (v_{12} + v_{13})S_g / S_{sb} = (x_2 / x_3 v_{13} + v_{13})S_g / S_{sb} = (x_2 + x_3) / x_3 v_{13} S_g / S_{sb}$.

Velocity $v_9 = v_{13} S_g / S_{sb}$.

We also denote the following velocity ratios:

$w_1 = v_7 / v_6 = (v_{11} + v_{12} + v_{13}) / (v_{10} + v_{11} + v_{12} + v_{13}) = (x_1 v_{10} + x_2 v_{10} + x_3 v_{10}) / (v_{10} + x_1 v_{10} + x_2 v_{10} + x_3 v_{10}) = (x_1 + x_2 + x_3) / (1 + x_1 + x_2 + x_3)$,

$v_{10} S_g / v_6 S_{sb} = v_{10} S_g / (v_{10} + v_{11} + v_{12} + v_{13})S_g = v_{10} / (v_{10} + x_1 v_{10} + x_2 v_{10} + x_3 v_{10}) = 1 / (1 + x_1 + x_2 + x_3)$,

$$v_{10}/v_6 = S_{sb}/S_g/(1+x_1+x_2+x_3),$$
$$v_{11}S_g/v_7S_{sb} = v_{11}S_g/(v_{11}+v_{12}+v_{13})S_g =$$
$$= x_1v_{10}/(x_1v_{10}+x_2v_{10}+x_3v_{10}) = x_1/(x_1+x_2+x_3),$$
$$v_{11}/v_7 = S_{sb}/S_g x_1/(x_1+x_2+x_3),$$
$$w_3 = v_9/v_8 = v_{13}/(v_{12}+v_{13}) = x_3v_{10}/(x_2v_{10}+x_3v_{10}) =$$
$$= x_3/(x_2+x_3),\ v_{12}S_g/v_8S_{sb} = v_{12}S_g/(v_{12}+v_{13})S_g =$$
$$= x_2v_{10}/(x_2v_{10}+x_3v_{10}) = x_2/(x_2+x_3),\ v_{12}/v_8 =$$
$$= S_к/S_n x_2/(x_2+x_3).$$

All velocity ratios in (16), (17), (20) and (21) are known. Let us introduce the following notation $x_1 = x_2 = x_3 = 1$, where $w_1 = w_2 = w_3 = 0.5$, $\zeta_7 = \zeta_8 = \zeta_9 = 0.4$, $\zeta_{10} = \zeta_{11} = \zeta_{12} = 0.552788$, cm. Formulas (18) and (19). Results of the filling of volume of H_0 height: $\mu_{1-10(10)} = 0.457672$, $v_{10} = 1.352335$ m/s, $\mu_{1-11(11)} = 0.4328906$, $v_{11} = 1.12603$ m/s, $\mu_{1-12(12)} = 0.422983$, $v_{12} = 0.895871$, m/s, $\mu_{1-13(13)} = 0.429016$, $v_{13} = 0.659530$ m/s, $x_1 = v_{11}/v_{10} = 0.822728$, $x_2 = v_{12}/v_{10} = 0.662462$, $x_3 = v_{13}/v_{10} = 0.487697$. Let us denote $x_1 = 0.822728$, $x_2 = 0.662462$, $x_3 = 0.487697$ and recalculate. Through consecutive approximations, we determine that $x_1 = 0.827696$, $x_2 = 0.491388$, $x_3 = 0$, and the time to fill a part of the mould with the height H_0 by the gates I – IV is 30.591 s.

We calculate the filling of the remaining volumes of the mould in a similar way. The results are shown in (Table 6). When filling in the volume between gates I and II $x_1 = 0.956$, $x_2 = 0.598$, $x_3 = 0$, between gates II and III – $x_1 = 1.137$, $x_2 = 0.963$, $x_3 = 0$, between gates III and IV – $x_1 = 1.166$, $x_2 = 1.308$, $x_3 = 0.687$.

Table 6 – Specifications of the gating system with gates I – IV

Parameters	Sections filled			
	0–I	I–II	II–III	III–IV
$\zeta_{1-10(10)}$	1.884	2.127	3.119	5.367
$\mu_{1-10(10)}$	0.589	0.558	0.493	0.396
v_{10}, m/s	1.740	1.540	1.155	0.724
$\zeta_{1-11(11)}$	2.186	2.046	2.187	3.682
$\mu_{1-11(11)}$	0.560	0.573	0.556	0.462
v_{11}, m/s	1.440	1.473	1.313	0.845
$\zeta_{1-12(12)}$	5.136	4.294	2.622	2.721
$\mu_{1-12(12)}$	0.404	0.435	0.525	0.518
v_{12}, m/s	0.855	0.921	1.113	0,947
$\zeta_{1-13(13)}$	∞	∞	∞	8.533
$\mu_{1-13(13)}$	0	0	0	0.324
v_{13}, m/s	0	0	0	0.498
Q, cm^3/s	258.43	251.92	229.35	193.04
v_{11}/v_{10}	0.828	0.956	1.137	1.166
v_{12}/v_{10}	0.491	0.598	0.963	1.308
v_{13}/v_{10}	0	0	0	0.686
τ, s	30.591	30.117	33.080	39.303

Mould filling time – 133.091 s

Research results and discussion

When there is only one gate in the system, the flow rate is the same both when the liquid is poured from top to bottom into the mould and when the mould is filled to a flooding level. For example, when gate I is operating, the flow rate is

0.769 when pouring from the top and filling under a flooding level between gate I and II, II and III, III and IV.

If there are more than one gate in GS, then in the gating system I–III, when filling the volume 0-I when pouring from the top $\mu_{1-10(10)} = 0.590$, $\mu_{1-11(11)} = 0.562$, $\mu_{1-12(12)} = 0.395$, when filling the volume I–II – 0.559, 0.575, 0.425 respectively, for volume II–III – 0.496, 0.563, 0.513, and for volume III–IV – 0.466, 0.534, 0.565. The flow rate for gate I decreased by 1.20 times and forgate III by 1.43 times. That is, the flow rate of gate I has decreased more slowly than the flow rate of gate III has increased.

It is evident that filling the mould with liquid under a flooded level through stepped gates located at different heights can be calculated. Before the gate slot is flooded with a rising molded liquid, the flow out of the gate occurs at a constant head, and after flooding, the flow out of the gate occurs at a variable head, the value of which is calculated using the formula for the calculated head. For each volume, there is a different design head between the gates, and the relation between the velocities in the gates when the volume is filled is by successive approximations. And these relations increase as the fluid changes its volume. And when filling the volume between gates III and IV in GS I–IV, the velocity in gates II and III is 1.166 and 1.308 times higher respectively. Although gates II and III are 119 and 238 mm higher than gate I, which looks incomprehensible and contradicts the theory of moulding.

In the multi gated system, as the liquid level rises in the mould, the resistance to branching off part of the flow from the vertical sprue to the first gate increases. For the system of I–IV gates, when pouring from the top $\zeta_{10} = 0.692$, $\zeta_{10} = 0.807$, 1.118 and 1.894 respectively when filling the I–II, II–III and III–IV volumes. And on passage from section 6–6 to section 7–7 resistance decreases when pouring from the top: $\zeta_7 = 0.230$;, 0.091 and 0.040 at filling of volumes I–II, II–III and III–IV. It is not clear what causes the increase in and decrease in. After all, the pressure above gate I increases both in the moulding and in the vertical basin, and the liquid level in the basin is higher than in the mould.

When all four gates are operating, when pouring liquid from the top to the mould and filling in volumes I–II and II–III, water from the top (fourth) gate does not flow, although the water level in the mould is 132.5 mm above the centre of the opening of gate IV.

Conclusion

Therefore, for the first time, it was possible to calculate the filling of the mould with metal under a flooded level through a stepped gate system. The filling of each mould volume between gates is calculated separately. The resistance coefficients, flow ratios of all operating gates and the flow rate of liquid from the gates vary as the metal level rises in the mould. However, the use of calculated head and the method of sequential approximations in calculating velocity ratios has made it possible to calculate the filling of mould sections between gates and the entire mould even for a complex system such as a step system in which gates are located at different heights in the mould.

The students R. Lukoyanov and E. Khoroshchy participated in the project.

References:

1. Васенин В. И. Особенности расчета расхода металла в литниковых системах // Известия высших учебных заведений. Машиностроение. 1988. – № 1. – С. 103–106.
2. Васенин В. И. Расчет расхода металла в разветвленной литниковой системе // Литейное производство. 2007. – № 4. – С. 5–8.

3. Vasenin V. I., Bogomyagkov A. V., Sharov K. V. Research of cross gating system // Science and Education: materials of the III international research and practice conference, Vol. I.– Munich: Vela Verlag, 2013.– P. 184–194.
4. Vasenin V. I., Bogomyagkov A. V. Investigation of the work on the P-shaped gating system // Austrian Journal of Technical and Natural Sciences.2017.– No. 1–2.– P. 38–50.
5. Васенин В. И., Богомягков А. В., Шаров К. В. Исследования кольцевых литниковых систем // Известия Самарского научного центра Российской академии наук.2013.– Том 15.– № 4 (2).– С. 316–322.
6. Vasenin V. I., Bogomyagkov A. V. The study of the work of the double-ring-shaped gating system / Science, Technology and Higher Education: materials of the XIII international research and practice conference.– Westwood (Canada): Accent Graphics communications, 2017.– P. 76–99.
7. Vasenin V. I., Bogomyagkov A. V., Sharov K. V. Research of gating system with collector of variable cross-section // Science, Technology and Higher Education: materials of the II international research and practice conference, Vol. II.– Westwood (Canada): Accent Graphics communications, 2013.– P. 250–260.
8. Vasenin V. I., Bogomyagkov A. V., Sharov K. V. Investigation del metallo liquido riempire lo stampo di colata con un sistema a canali conico // Italian Science Review.2014.– No. 4 (13).– P. 147–159.– URL: http://www.ias-journal.org/archive/2014/april/VaseninV.pdf
9. Vasenin V. I., Bogomyagkov A. V. Study of gating system with two sprues // Eastern European Scientific Journal.2018.– No. 3.– P. 410–419.
10. Vasenin V. I., Bogomyagkov A. V. Study of the work on the gating system with sprues of different height / / Austrian Journal of Technical and Natural Sciences.2018.– No. 7–8.– P. 20–28.
11. Vasenin V. I., Bogomyagkov A. V., Sharov K. V. Step gate investigation // Science and Education: materials of the III international research and practice conference, Vol. I.– Munich: Vela Verlag, 2013.– P. 194–205.
12. Vasenin V. I., Bogomyagkov A. V., Sharov K. V. Investigation into a storeyshaped gating system // Eastern European Scientific Journal.2014.– No. 4.– P. 122–137.
13. Vasenin V. I., Bogomyagkov A. V., Sharov K. V. Investigating work of vertical double-ring-shaped gating system // Eastern European Scientific Journal.2019.– No. 4.– P. 26–40.
14. Vasenin V. I., Bogomyagkov A. V., Sharov K. V. Study of the combined operation of the ring-shaped gating system and the step gating system // Austrian Journal of Technical and Natural Sciences.2019.– No. 1–2.– P. 10–19.
15. Vasenin V. I., Bogomyagkov A. V., Sharov K. V. Research of the ring and branched gating systems joint operation // Eastern European Scientific Journal.2019.– No. 3.– P. 5–20.
16. Меерович И. Г., Мучник Г. Ф. Гидродинамика коллекторных систем.– М.: Наука, 1986.– 144 с.
17. Чугаев Р. Р. Гидравлика.– М.: изд-во "Бастет", 2008.– 672 с.
18. Токарев Ж. В. К вопросу о гидравлическом сопротивлении отдельных элементов незамкнутых литниковых систем // Улучшение технологии изготовления отливок.– Свердловск: изд-во Уральского политехнического института, 1966.– С. 32–40.
19. Jonekura Koji (et al.) Calculation of amount of flow in gating systems for some automotive castings // The Journal of the Japan Foundrymen's Society.1988.– Vol. 60.– No. 8. – P. 326–331.
20. Идельчик И. Е. Справочник по гидравлическим сопротивлениям.– М.: Машиностроение, 1992.– 672 с.

21. Васенин В. И., Васенин Д.В, Богомягков А. В., Шаров К. В. Исследование местных сопротивлений литниковой системы // Вестник Пермского национального исследовательского политехнического университета. Машиностроение, материаловедение.– 2012.– Т. 14.– № 2.– С. 46–53.
22. Штеренлихт Д. В. Гидравлика.– М.: Энергоатомиздат, 1984.– 640 сс
23. Васенин В. И., Голубцов С. А. Определение напора и суммарной площади питателей литниковой системы // Вестник Пермского государственного технического университета. Машиностроение, материаловедение.– 2007.– № 3 (10).– С. 76–81.
24. Васенин В. И., Богомягков А. В., Шаров К. В. Исследования L-образных литниковых систем // Вестник Пермского национального исследовательского политехнического университета. Машиностроение, материаловедение.– 2012.– Т. 14.– № 4.– С. 108–122.

Section 5. Mechanics

https://doi.org/10.29013/AJT-20-9.10-36-38

Solodei Ivan,
DSc, Department of Structural mechanics,
Kyiv National University of Construction and Architecture,
Kyiv, Ukraine
Zatyliuk Gherman,
Postgraduate student, Department of Structural mechanics,
Kyiv National University of Construction and Architecture,
Kyiv, Ukraine
E-mail: zatyliuk.ha@knuba.edu.ua

MOHR-COULOMB MODEL WITH CORRECTED PARAMETERS IN THE STUDY OF BASE SETTLEMENTS

Abstract. The article describes a technique for investigating base settlements using the Mohr–Coulomb soil model with corrected parameters. The formulas for changing the deformation modulus with depth are derived, which are based on the relations between the deformation characteristics of the soil and the level of stresses in the array used in the Hardening Soil Model.

Keywords: underground structure, soil mass, base settlements, computational area limit, Mohr–Coulomb model, Hardening Soil Model.

One of the most common issues in numerical modelling of "underground structure — soil body" system is selection of boundaries of calculation area. The question of choice of the lower boundary of the model is especially important, if the object of study is precipitation. It is known that the values of this type of deformations will grow along with increasing model depth (vertical dimensions).

One of the possible solutions is to limit the model size so that the influence of boundary conditions on force distribution is minimal [1]. This approach has been used, for example, in works [2; 3].

This method actually consists in removal of numerical model boundaries from underground structure, and, consequently, it is unacceptable for study of settlement deformations, because increase of model lower boundary depth, on the one hand, reduces influence of boundary conditions on stress state and, on the other hand, leads to unjustified increase of deformations.

In this case, it is possible to use another method [1, 4] to limit the computational pattern to the depth of compressible thickness, which is calculated by layered summation method, the boundary of which is at the depth where the condition is met:

$$\sigma_{zp} \le 0,2\sigma_{zg}, \quad (1)$$

where σ_{zg} is the dead load stress of the soil;

σ_{zp} is the pressure from the structure, taking into account the depth attenuation ratio a.

This approach is often used in design practice and described in work [5].

However, often, due to the specifics of the studied objects, it is impossible to use the recommendation to limit the computational pattern to the depth of compressible thickness. That is why the question of development of algorithms for modelling of "underground structure - soil body" system in program complexes and adjustment of input parameters so that the value of settlement at static calculation would be identical irrespective of chosen lower boundary of calculation model and would be close to the values of settlement calculated by classical analytical methods is relevant.

We have developed and described the approach to modelling of the system "underground structure - soil body", which would be deprived of drawbacks of rapid proportional growth of settlement at increasing of depth of the lower boundary of the model, using possibility of introduction of additional parameters for the Mohr–Coulomb model in Plaxis [6].

The method was based on the possibility to set additional parameters for the Mohr–Coulomb model in Plaxis, namely, to set the deformation modulus, which increases linearly with the depth – $E_{increment}$ [kPa/m]. Accordingly lower than z_{ref} (in Plaxis –yref) depth, the deformation modulus is the sum of the normative value of the deformation modulus Ei (in Plaxis – E_{ref}) and the depth increment:

$$E_{z,i} = E_i + E_{increment} \cdot (z - z_{ref}) \qquad (2)$$

Changing the deformation modulus was based on the theory of linear-deformed medium, according to which the normal stresses under the rectangular platform, which exerts pressure, varies with the depth by a rule (3):

$$\sigma = \frac{2 \cdot p}{\pi}\left(arctg\left(\frac{\eta}{\zeta \cdot \sqrt{1+\zeta^2+\eta^2}}\right) + \frac{\zeta \cdot \eta \cdot (1+\eta^2+2\zeta^2)}{(\eta^2+\zeta^2)\cdot(1+\zeta^2)\cdot\sqrt{1+\zeta^2+\eta^2}}\right), \qquad (3)$$

where η is the ratio of sides of the site, and ζ is the relative depth to the width of the site:

$$\eta = \frac{l}{b}, \qquad (4)$$

$$\zeta = \frac{2z}{b}, \qquad (5)$$

where l and b are the length and width of the site respectively;

z is the depth at which the stress is determined.

The above approach is based on the theory of linearly deformed medium, which does not take into account soil parameters. Another approach may be to use dependencies used in the Hardening Soil Model. For example, in article [7] the soil model is broken down into layers, the deformation modulus for each is calculated using formula (6).

The dependences of deformation characteristics in the Hardening Soil Model depend on the stress level and are described by the formula ("–" symbol before σ_3 is replaced by "+"):

$$E = E^{ref}\left(\frac{c\cos\varphi + \sigma_3 \sin\phi}{c\cos\varphi + p^{ref}\sin\phi}\right)^m, \qquad (6)$$

where c is the specific cohesion of the soil;

φ is the internal friction angle;

m is the soil stiffness index, sets the curvature of the relation;

p_{ref} is the reference pressure, is an input parameter of the model;

Eref is the deformation modulus (three different modulus are used in the HSM model), determined by comprehensive compression pref, are the input parameters of the model (in formula (2) is designated *Ei*).

In fact, with increasing depth, the stress $\sigma 3$, respectively, with increasing depth, the modulus E, as Ez.i increases in formula (2).

Having equated (2), (6) and having got rid for the further transformations from an index power m, we obtain:

$$E^{ref} + E_{increment} \cdot (z - z_{ref}) = E^{ref}\left(\frac{c\cos\varphi + \sigma_3\sin\varphi}{c\cos\varphi + p^{ref}\sin\varphi}\right)^m, \qquad (7)$$

$$\frac{E_{increment} \cdot (z - z_{ref})}{E^{ref}} = \frac{c\cos\varphi + \sigma_3\sin\varphi}{c\cos\varphi + p^{ref}\sin\varphi} - 1, \qquad (8)$$

$$\frac{E_{increment} \cdot (z - z_{ref})}{E^{ref}} = \frac{\sigma_3 - p^{ref}}{c \cdot ctg\varphi + p^{ref}} \qquad (9)$$

Introducing the side pressure coefficient K_0, and expressing the stress in the mass through the multiplication of soil density γ and depth z, we obtain:

$$\frac{E_{increment} \cdot (z - z_{ref})}{E^{ref}} = \frac{z - z_{ref}}{\frac{c \cdot ctg\varphi}{\gamma \cdot K_0} + z_{ref}} \qquad (10)$$

Therefore:

$$E_{increment} = \frac{E^{ref}}{\frac{c \cdot ctg\varphi}{\gamma \cdot K_0} + z_{ref}} \qquad (11)$$

Now, in the Plaxis window of additional parameters for the Mohr-Coulomb model, a deformation modulus can be specified $E_{increment}$, that increases linearly with depth, having previously found it by formula (11).

The ability of soils and a direct correlation between the deformation modulus and the stress level in the soil mass). In practice, for the Hardening Soil model m is taken in the range of 0.5 ... 1, because at values less than 0.5 it is not reasonable to use such a complex model.

For better convergence, it is suggested to enter this value into formula (11):

$$E_{increment} = \frac{E^{ref} m}{\frac{c \cdot ctg\varphi}{\gamma \cdot K_0} + z_{ref}} \qquad (12)$$

Taking into account the non-regulation of the domestic norms of parameter m determination, it is recommended to use the value m = 0.5 as the smallest one, which is reasonable to use.

The described technique requires verification to determine the possibility of its practical use by solving a number of test examples and comparing settlement values when solving problems with its use, using techniques [6; 7], using the Hardening Soil Model. Also, the obtained precipitation should be compared with the solution obtained using the layered summation method, which is widely used in the calculation of base settlements.

References:

1. Perelmuter A. V., Slivker V. I. Design models of structures and the possibility of their analysis.– Moscow: SKAD SOFT, 2011.– 736 p. [in Russian].
2. Berezhnoy D. V., Sagdatullin M. K., Sultanov L. U. Choosing a soil model for numerical simulation of the influence of deep excavation on the existing building. Bulletin of Kazan Technological University. 2013.– No. 9.– P. 250–255. [in Russian].
3. Petrov D. N., Demenkov P. A., Potemkin D. A. Numerical modeling of the stress state in the lining of columnar stations without side platforms. Notes of the Mining Institute. 2010.– 185.– P. 166–170. [in Russian].
4. Gorodetskiy A. S., Evzerov I. D. Computer models of designs.– Kyiv: Fakt, 2009.– 360 p. [in Russian].
5. Ryabkov S. V., Soloviev R. A. Experience of using the Plaxis 3D software package by the design department of tunnel building structures // Subways and tunnels. 2019.– No. 6.– P. 53–55. [in Russian].
6. Solodei I., Zatyliuk Gh. Implementation of the linear elastic structure half-space in the Plaxis in the study of settlements // Proceedings of Odessa Polytechnic University. 2019.– No. 1(57).– P. 22–28.
7. Holubev A. I., Seletskii A. V. The choice of soil model and its parameters in the calculation of geotechnical objects // The Proceedings of the International Conference in Geotechnics GeoMosю 2010.– 4.– P. 1727–1732. [in Russian].

Section 6. Agricultural sciences

https://doi.org/10.29013/AJT-20-9.10-39-43

Zaiets Sergiy Oleksandrovych,
Candidate (Ph.D.) of Agricultural Sciences,
Institute of Irrigated Agriculture of NAAS
E-mail: szaiets58@gmail.com

Kysil Liudmyla Bohdanivna,
Ph.D. student, and Non-irrigated Agriculture
of the Institute of Irrigated Agriculture of NAAS
E-mail: lkisiel@ukr.net

Lykhovyd Pavlo Volodymyrovych,
Candidate (Ph.D.) of Agricultural Sciences,
Institute of Irrigated Agriculture of NAAS
E-mail: pavel.likhovid@gmail.com

WATER USE OF BARLEY VARIETIES DEPENDING ON SOWING DATES AND GROWTH REGULATORS IN THE CONDITIONS OF IRRIGATION IN THE SOUTHERN STEPPE OF UKRAINE

Abstract. Typical winter variety of barley Academichnyi and alternate variety Deviatyi Val were studied under sowing on October 1st and 20th, at treatment of the seeds and plants with growth regulators Humifield Forte Brix, MIR and PROLIS. Academichnyi variety needed 48–71 m^3/ha more water for seed formation if sown on October 1st, and 3–20 m^3/ha less than Deviatyi Val variety if sown on October 20th. The work scientifically substantiates and proves that the most effective water use was recorded in the variety deviatyi Val at sowing on October 1st and seed treatment with Humifield (0.8 L/t), MIR (6 g/t) and PROLIS (5 g/t), where the total water use was 2706, 2715 and 2718 m^3/ha, and water use per 1 ton of grain – 390, 386 and 391 m^3.

Keywords: winter barley, variety, sowing date, growth regulators, water use.

Introduction. Barley grain takes one of the important places in the world balance of the grain production. In terms of sown area and gross grain yield, it occupies the fourth place in the world after wheat, rice and corn, and in Ukraine – the second place after wheat [1; 2].

Nowadays, barley grain is in great demand and at a high price on the world market. In this regard, Ukraine has great potential for barley grain production and opportunities to increase its exports and earn significant funds from it. And first of all it is necessary to expand the sowing area of winter barley, which is more productive, than spring one [3].

At the same time, the yield of winter barley in the Southern Steppe of Ukraine remains low (3.4 t/ha)

and fluctuates greatly over the years [4]. One of the reasons for this is that changes in weather and climatic conditions, features of zonal and varietal technology of its cultivation, and, first of all, modern high-yielding varieties, terms of their sowing and preparations that increase winter tolerance of plants are not taken into account.

In the conditions of arid climate and moisture deficit in the Southern Steppe of Ukraine, winter barley can open its productive potential only under the irrigated conditions. Therefore, the cultivation technology of new winter barley varieties at irrigation, considering the emergence of new high-yielding varieties, innovative growth regulators and climate change, needs detailed research and improvement.

Analysis of literature, problem statement. In the recent years, there have been significant fluctuations in meteorological indices in the Southern Steppe of Ukraine due to the climate change, which is mainly associated with the phenomenon of global warming [5; 6]. Thus, the average annual air temperature for the last fifty years in this zone has increased by 1.8 °C, and in June and August by 3.1–3.9 °C, reaching the maximum daily average in August – 24.8 °C [7]. Besides, an increase is observed in the spring, especially in March – by 2.3 °C, as well as in September and October – by 2.0 and 1.4 °C, respectively. At the same time, there was a significant decrease in precipitation in 2011, 2012, 2013, 2014, 2017 and 2018, in which its amount was 314.4 mm, 369.9, 332.9, 363.5, 310.0 and 409.4 mm, respectively, while the average for 50 years is 444.9 mm. In 2010, 2015, 2016 and 2019, the amount of precipitation increased, but it was mainly because of showers occurrence and its distribution was significantly uneven during the growing season.

Such agrometeorological conditions significantly affect the water supply of plants, their growth and development and formation of grain yield. Therefore, studies on water use of new high-yielding varieties and, first of all, at different sowing dates and growth regulators application on the irrigated lands of the Southern Steppe of Ukraine are quite relevant.

Aim of the study – to investigate the influence of sowing dates and growth regulators on the total water use and water use per 1 ton of grain of new winter barley varieties on the irrigated lands of the Southern Steppe of Ukraine.

Tasks and methods of the study. Field experiments were conducted during 2015–2019 at the Institute of Irrigated Agriculture of NAAS, which is located in the area of the Ingulets irrigation system. The soil is typical for the irrigated lands of the Southern Steppe of Ukraine and is represented by the dark-chestnut middle-loamy slightly-saline soil. The forecrop for winter barley was soybean (early-ripening variety Diona). The experiments were conducted with accordance to the generally accepted cultivation technology of winter barley in the Southern Steppe of Ukraine, excepting technological measures that were studied. Observations, analyzes and records were performed in accordance with the methods of the field and laboratory experiments on the irrigated lands [8].

The study was performed using typically winter variety of barley Academichnyi and the alternate variety Deviatyi Val (factor A), which are included in the State Register of Plants and Varieties Suitable for Use in the Steppe in 2011 and 2015, respectively [9]. Sowing was carried out in two dates: October 1st and 20th (factor B). The seeds were treated with growth regulators Humifield Forte Brix (0.8 L/t), MIR (6 g/t) and PROLIS (5 g/t) before sowing (factor C) and the crops were additionally treated through spraying with these preparations (respectively, 0.4 L/ha, 6 g/ha and 2 g/ha) in the early spring.

Humifield Forte Brix contains 60 g/L of seaweed extract and 135 g/L of humic acid salts, incl. amino acids – 20 g/L, potassium (K_2O) – 20 g/L and trace elements – 5 g/L. It has a complex effect on the plant as an anti-stress and growth stimulator [10]. *MIR* – multi-purpose immunoregulator of growth is created on the basis of synthetic compounds and has a wide range of microelements in a chelatic form [11].

PROLIS – L-*a* proline aminoacid. PROLIS is used to prepare plants for winter, in order to repair them after winter and avoid the effects of negative environmental factors: cold, frost, drought, waterlogging. The preparation is intended for biotic and abiotic reduction of plant stress. It regulates the assimilation of macro-and micronutrients, as well as stimulates the immune system of plants, significantly increases plant productivity and crop quality [12].

Soil moisture in the plots was determined to the depth of 1.0 m by gravimetric method in two non-adjacent repetitions. The total water use for the spring-summer growing season was determined by the method of water balance. The water use coefficient was calculated as a ratio of the total water use during the growing season to the grain yield of winter barley.

Discussion of the study results. The results of the study discovered that the water use of new winter barley varieties by each year had its own peculiarities. An important role is played by pre-sowing soil tillage and sowing conduction. In most cases, after harvesting the forecrop and the initial period of autumn vegetation, soil moisture supply is unfavorable for obtaining sprouts timely, in this period there is the greatest deficit of soil moisture in the Southern Steppe of Ukraine. Therefore, to obtain complete sprouts and good condition of the crops before the winter period, in the autumn of 2017 and 2018 it was necessary to conduct water-charging (500 and 400 m^3/ha), and in 2017 additional sprout-provoking (250 m^3/ha) watering.

To maintain the moisture content in the soil layer of 0–50 cm at the level of 70% FC in the spring-summer growing season in 2017, the crops required two vegetative irrigations at a rate of 400 m^3/ha each, and in 2018 – three irrigations with a total irrigation rate of 1350 m^3/ha. This allowed to form a well-developed green mass with a sufficient number of productive stems. In the spring vegetation period of 2019, there was 136.1 mm of precipitation, which is almost one and a half times higher than the average long-term values. Therefore, in such humid weather conditions, there was no need for vegetative watering.

The study has determined that due to significant rainfall the total water use of winter barley in 2019 was the greatest and averaged to 2833–3295 m^3/ha, and the lowest it was in 2017–2271–2481 m^3/ha (Table 1).

Table 1. – Winter barley water use from the meter soil layer depending on the variety and growth regulators (average for 2016–2019)

Variety (A)	Sowing date (B)	Growth regulators (C)	Total water use, m^3/ha			
			2017	2018	2019	average
1	*2*	*3*	*4*	*5*	*6*	*7*
Academichnyi	October 1st	Control	2481	2784	2945	2737
		Humifield (seeds)	2481	2796	3029	2769
		MIR (seeds)	2481	2788	3043	2771
		PROLIS (seeds)	2481	2788	3029	2766
		Humifield (plants)	2481	2794	3057	2777
		MIR (plants)	2481	2793	3036	2770
		PROLIS (plants)	2481	2786	3022	2763
	October 20th	Control	2313	2715	3211	2746
		Humifield (seeds)	2313	2727	3267	2769
		MIR (seeds)	2313	2725	3281	2773
		PROLIS (seeds)	2313	2723	3288	2775
		Humifield (plants)	2313	2725	3281	2773
		MIR (plants)	2313	2719	3288	2773
		PROLIS (plants)	2313	2718	3295	2775

1	*2*	*3*	*4*	*5*	*6*	*7*
Deviatyi Val	October1st	Control	2397	2818	2833	2683
		Humifield (seeds)	2397	2831	2889	2706
		MIR (seeds)	2397	2831	2917	2715
		PROLIS (seeds)	2397	2832	2924	2718
		Humifield (plants)	2397	2833	2889	2706
		MIR (plants)	2397	2831	2903	2710
		PROLIS (plants)	2397	2837	2917	2717
	October 20th	Control	2271	2801	3225	2766
		Humifield (seeds)	2271	2807	3239	2772
		MIR (seeds)	2271	2812	3253	2779
		PROLIS (seeds)	2271	2815	3267	2784
		Humifield (plants)	2271	2814	3260	2782
		MIR (plants)	2271	2805	3253	2776

On average, in 2016–2019, the total water use of Academichnyi winter barley variety from a meter layer of soil ranged from 2737 to 2777 m^3/ha, and of the variety Deviatyi Val – from 2683 to 2784 m^3/ha. The total water use of winter barley varieties was slightly different. Thus, the variety Academichnyi required 48–71 m^3/ha more water for the seed formation at sowing on October 1st, and 3–20 m^3/ha less than the variety Deviatyi Val at sowing on October 20th, due to their varietal features.

Biological properties of the varieties had different water demand depending on the sowing date. Academichnyi variety plants had minimal difference in total water use by the date of sowing, or used almost the same amount of moisture per unit area, while Deviatyi Val required 55–83 m^3/ha more water of sown on October 20th.

The value of the total water use of winter barley varieties was also affected by the application of growth regulators. They contributed to a better formation of vegetative mass of the plants, resulting in the consumption of a significant volume of water and, as a result, increased the total water use by 23–40 m^3/ha in the variety Academichnyi and by 6–35 m^3/ha for the variety Deviatyi Val.

The highest values of the total water use of 2782–2784 m^3/ha were recorded for the variety Deviatyi Val at sowing on October 20th and application of PROLIS preparation for the seed treatment and Humifield spraying of the plants. In the variety Academichnyi the highest total water use of 2777 m^3/ha was also recorded under spraying the plants with the growth regulator Humifield, but at sowing on October 1st.

Application of the growth regulators led to the lowest total water use (2706 m^3/ha) on the variety Deviatyi Val at sowing on October 1 and treatment of the seeds and plants with Humifield, and on the variety Academichnyi (2763 m^3/ha) – at sowing in the same term and spraying the plants with PROLIS preparation.

Due to higher productivity on the variants with application of the growth regulators, water per unit of the yield was used more economically. Thus, at their application the coefficient of water use of the varieties on average over the years of the study was 386–515 m^3/t while without them – 413–538 m^3/t.

Deviatyi Val used water per the unit of grain more economically. At sowing of this variety on October 1st, the most efficient water use was in the variant of the seed treatment with MIR, Humifield and PROLIS – 386, 390 and 391 m^3/t, respectively, which is 27, 23 and 24 m^3/t less than in the control variant.

At sowing on October 1st, the variety Academichnyi showed the best performance when Humifield and MIR were applied, both for the seed and plant treatment – 420 and 422 and 425 and 426 m^3/t,

respectively, as well as the seed treatment with PROLIS – 428 m^3/t. At sowing on October 20th, due to lower yields, the water use coefficient was higher, but also all the growth regulators contributed to the economical use of water – 502–515 m^3/t, which is 23–36 m^3/t less than in the control variant.

Analysis of the balance of the total water use in 2016/17 and 2017/18 for the spring-summer growing season of winter barley varieties testifies that when growing them after soybean in the irrigated conditions, on average by factor C (growth regulators), the share of soil moisture was 19.0–22.9%, precipitation – 36.8–39.2% and irrigation – 40.2–42.1%.

That is, the total water use of winter barley varieties depended on irrigation and precipitation during the growing season.

Conclusions. Thus, among the studied varieties, the best water use efficiency was observed for the variety Deviatyi Val at sowing on October 1st and seed treatment with Humifield (0.8 L/t), MIR (6 g/t) and PROLIS (5 g/t), where the total water use was 2706, 2715 and 2718 m^3/ha, and water use per 1 ton of grain – 390, 386 and 391 m^3. The variety Academichnyi formed slightly lower grain productivity than Deviatyi Val, so its total water use at sowing on October 1st and seed treatment with Humifield, MIR and PROLIS, as well as at spraying the plants with Humifield and MIR were 2769, 2771, 2766, 2777 and 2770 m^3/ha, respectively, and the water use coefficient was 420, 426, 428, 422 and 425 m^3/t.

References:

1. Barley cultivation in the world. URL: https://www.yara.ua/crop-nutrition/barley/barley-key-facts/barley-world-production
2. Manko K., Muzafarova N. Spring barley: modern cultivation technologies. Agronomy Today. 2012. URL: http://agro-business.com.ua
3. Buchynskyi I. Ye. Climate of Ukraine in the past, present and future.– Kyiv, 1963.– 308 p.
4. Karazhbei G. State and prospects of winter barley on the seed market of Ukraine. 2018. URL: https://infoindustria.com.ua/stan-ta-perspektivi-yachmenyu-ozimogo-na-nasinnyevomu-rinku-ukrayini
5. Netis I. T. Winter wheat in the South of Ukraine: monograph. – Kherson, 2011.– 460 p.
6. Zaiets S. O., Netis V. I. Water use of cereals and soybean depending on water supply conditions. Irrigated Agriculture. 2013.– Vol. 59.– P. 30–34.
7. Kovalenko A. M., Kiriyak Yu. P. Winter wheat wintering conditions in the Southern Steppe zone of Ukraine in the context of climate change. Irrigated Agriculture. 2016.– Vol. 66.– P. 34–38.
8. Vozhehova R. A. Methods of field and laboratory experiment on the irrigated lands; Eds.– Kherson. 2014.– 286 p.
9. State Register of Plant Varieties Suitable for Distribution in Ukraine for 2017. State Veterinary and Phytosanitary Service of Ukraine.– Kyiv. 2017.– 390 p.
10. Humifield, Humifield Forte, Fulvital Plus. Brochure. Agrotechnosoyuz.– Kyiv, 2015.– 32 p.
11. Plant growth regulator MIR mark 3. Agrarians together. URL: https://agrarii-razom.com.ua/preparations/mir-marki-z
12. Prolis T. M. Plant growth regulator, B. Agrarians together. URL: https://agrarii-razom.com.ua/preparations/prolis-tm-vp

Section 7. Technical sciences

https://doi.org/10.29013/AJT-20-9.10-44-46

Sobirjonov Rakhmatjon Rustambek ugli,
PhD student, Academy of Sciences of the Republic of Uzbekistan Institute of General and inorganic chemistry
Khamidov Bosit Nabiyevich,
Doctor of technical Sciences, Professor,
Academy of Sciences of the Republic of Uzbekistan Institute of General and inorganic chemistry
Khujakulov Aziz Fayzullayevich,
PhD student, Academy of Sciences of the Republic of Uzbekistan Institute of General and inorganic chemistry, c. Tashkent
E-mail: raximov2021@inbox.ru

PRODUCTION OF THE OPTIMAL VERSION OF A PILOT BATCH OF PLASTICIZER OIL IN THE CONDITIONS OF THE FERGANA REFINERY

Abstract. In this work, the optimal version of the pilot batch of plasticizer oil was produced from the extract of III-pogon in the conditions of the Fergana oil refinery.

Keywords:

At present, in the oil and gas industry of the Republic of Uzbekistan, special attention is paid to the priority areas of oil and gas chemistry in order to implement industries that produce products with high added value, in particular, in this area there are opportunities for obtaining new types of products – polystyrene, polyethylene terephthalate, synthetic rubbers based on aromatic hydrocarbons (benzene, toluene, xylene), using the technology for producing olefins from methanol, as well as increasing the production of polyethylene and polypropylene.

According to the analysis of the state of work on plasticizers, petroleum oils and products based on them are widely used in the tire industry as plasticizers and softeners of rubber compounds, and in terms of the total volume of use they occupy the third place after rubbers and carbon black [1]. Petroleum plasticizers are especially widely used in the production of styrene butadiene rubbers and tire rubbers, into which petroleum oils are introduced in large quantities (20–50 mass parts or more per 100 mass parts of polymer). The viscoelastic, low-temperature strength properties of rubbers, as well as wear resistance, shrinkage, adhesion, tendency to vulcanization, and workability largely depend on the composition of the plasticizer [2].

The following requirements are imposed on the substances used as plasticizers: they must be well

combined with the polymer, have low vapor pressure, high chemical resistance, heat and light stability, not dissolve in water, detergent solutions, oils. In addition, they should be colorless, odorless, tasteless, non-toxic, non-flammable and, most importantly, inexpensive. A universal plasticizer that would have all of the listed properties does not yet exist. Depending on the field of application of the polymer and the requirements imposed, either one or a mixture of plasticizers is introduced into the composition of their compositions [3].

At present, the industry of the leading capitalist countries, as well as the neighboring countries, produces more than 40 types of plasticizers, about 100 more are produced in small quantities for special purposes. Of the large number of compounds, esters of various acids are most often used as plasticizers for polymeric materials. In particular, the longer the alkyl chain, the greater the effectiveness of dialkyl esters of phthalic acid; branched esters have a weaker plasticizing effect than linear ones. Plasticizers are also polymeric compounds, for example copolymers of isobutylene-butadiene-acrylonitrile, isobutylene-acrylonitrile-methyl methacrylate, butadiene-acrylate, butadiene with carbonyl-containing compounds, polymeric esters of unsaturated carboxylic acids, copolymers of unsaturated acid ester dicarboxylic esters and polyethers of dicarboxylic acid esters. Plastics of this group are distinguished by extremely low volatility and provide frost resistance and elasticity of products [4].

We have carried out work on the manufacture of a pilot batch of plasticizer oil. The preparation process for this pilot batch consisted of the following stages:

– preparation of the components of the residual extract and the extract of the III-shoulder strap;
– purification of oil extracts with liquid propane;
– mixing of components.

Samples from pilot production batches were taken and analyzed from the installation 36/1, the quality characteristics of which are shown in(table 1):

Table 1.

No.	The name of indicators	Residual extract	Extract III-shoulder
1.	Kinematic viscosity at 100 ˚C, sSt	20.61	8.21
2.	Flash point, ˚C	250	194
3.	Refractive index at 50 ˚C	1.5100	1.4920
5.	Density at 20 ˚C, kg/m^3	936	922
6.	Pour point, ˚C	34	25
7.	Sulfur content,% mass.	1.80	1.85
8.	Aniline point, ˚C	72.2	66.7

The prepared samples are shown in (table 2):

Table 2.

Component name	Sample 1	Sample 2	Sample 3
Fraction III extract	10%	15%	20%
Residual extract I	90%	85%	80%

The quality of the prepared plasticizer samples is in (table 3):

Table 3.

No.	The name of indicators	Plasticizer oil			
		Norm	Laboratory samples		
			No. 1	No. 2	No. 3
1.	Kinematic viscosity at 100 ˚C, mm^2/s (sSt)	16–23	19.53	18.25	15.27
2.	Refractive index at 50 ˚C	1.5080–1.5280	1.5110	1.5030	1.5010
3.	Density at 20 ˚C, kg/m^3	927–967	934	927	923
4.	Pour point, ˚C	not higher than 30	32	30	28
5.	Closed Cup Flash Point, ˚C	not lower than 220	245	235	224
6.	Sulfur content,% mass.	no more than 3.0	1.8	1.75	1.79
7.	Aniline point, ˚C	64–72	71.8	69.5	67.4

As a result of the tests, it was found that the obtained laboratory samples of the plasticizer oil meet the requirements of the standard indicators.

Thus, an experimental batch of plasticizer oil obtained under laboratory conditions of the Fergana refinery can be recommended for transfer to operational tests in the production of rubber products. Scientific and practical work in this direction continues.

References:

1. Information bulletin "Raw materials and materials of the tire industry".– Moscow, LLC "Institute of the tire industry", 2011.– 194 p.
2. Markova L. M. Research of oil refined products as plasticizers of rubbers and rubbers. Dissertation for the degree of candidate of technical sciences. MIOC and GP them. I. M. Gubkin. 1964.– 242 p.
3. Rabinovich V. Yu. Use of plasticizers for rubber and rubber-based resin. Dissertation for the preparation of a scholarly degree of technical science candidates. MIOC and GP them. I. M. Gubkin. 1975.– 306 p.
4. Erman Burak, James E. Mark, Roland C. Michael. The Science and Technology of Rubber.Fourth edition. Academic Press. 2013.– 256 p.

Section 8. Chemistry

https://doi.org/10.29013/AJT-20-9.10-47-52

Kodirov Abduakhad Abdurakhimovich,
PhD in chemistry, docent, Qarshi State University, Uzbekistan
E-mail: kodirov.abduaxad@mail.ru
Chuliyev Jamshid Ruzibayevich,
scientific researcher, Qarshi engineering- ekonomical institute
Mamarakhmonov Mukhamatdin Khomidovich,
PhD in chemistry, docent, department of chemistry,
Andijan State University, Uzbekistan, Andijan
E-mail: muhamatdin@mail.ru
Askarov Ibragim Rakhmanovich,
Doctor of chemical Sciences, professor, Department of Chemistry,
Andijan State University, Uzbekistan, Andijan
E-mail: stek@inbox.ru

SYNTHESIS, CRYSTAL STRUCTURE OF MONO- AND BIS *α*-AMINONITRILES AND CLASSIFIATION BASED ON CHEMICAL COMPOSITION

Abstract. This article presents the results of the synthesis of new derivatives of *α*-aminonitriles. As well as the physicochemical properties of the synthesis products were studied. The crystal structure of the synthesized products was confirmed by X-ray analysis. The chemical composition of the newly obtained products was studied and classified by digital brand codes.

Keywords: α-Aminonitriles, synthesis, anhydrides of acids, biological activity, IR-spectra, X-Ray, Chemistry of goods, classification, digital brand code.

Introduction

α-Aminonitriles are the subject of many scientific studies by chemists. This article solves the problems of synthesis of new biologically active compounds of *α*-aminonitriles, study of the spatial crystal structure and classification according to their chemical composition. By us synthesized some new products of α-aminonitriles. The classification of goods is done according to the methods of the new subject "Chemistry of goods", created in Uzbekistan in 2017.

Experimental

Impressive reagents in the reaction are α-amino nitriles, anhydrides of acids are taken in proportion 1:1 by moles, give mono acyl product, and reaction mainly goes to the free amino group. If reagents taken by 2:1 proportion, accordingly, observed that, reaction give bis-acyl product. In the first case, the

reaction proceeds well at room temperature, while in the second case, the reaction mixture must be heated to the boiling point of the reaction solvent in order to complete the reaction [1–3]. The reaction of N-mono(*α*-cyanisopropyl) ethylenediamine with benzoic acid anhydride is similar to its reaction with acetic acid anhydride. The formation of N-benzoyl-N'-(*α*-cyanisopropyl) ethylenediamine (I) with high yields was observed when the reactants were obtained in a 1: 1 molar ratio.

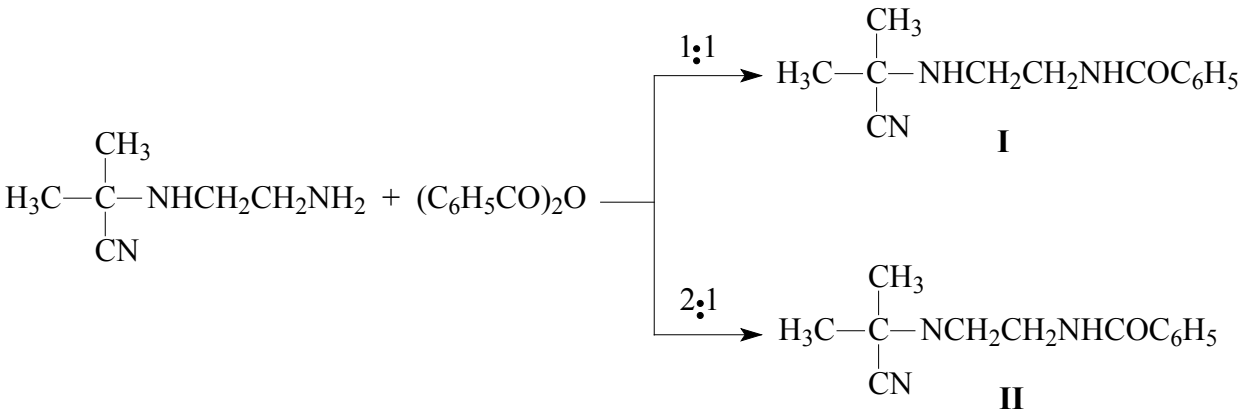

N, N'-dibenzoil-N- (*α*-cyanisopropyl)ethylenediamine (II) was formed with high yields when the reactants were obtained in a ratio of 1: 2 moles and the reaction was carried out at the boiling point of the solvent.

In the IR spectrum of the above compounds (I–II) the quantities corresponding to the absorption spectra of the aromatic ring are 1625–1575 cm^{-1}, and the absorption spectra of the NH- and CN-groups are 3320–3360 cm^{-1} and 2220–2231 cm^{-1} was found to be present [4–5].

In the mass spectra of these compounds, the presence of high percentages of the peak corresponding to the molecular ion intensity of the compounds was observed. For example, the molecular ionic peak intensity of N, N'-dibenzoil-N- (*α*-cyanisopropyl) ethylenediamine (II) was m/z 335, and its percentage was 21%.

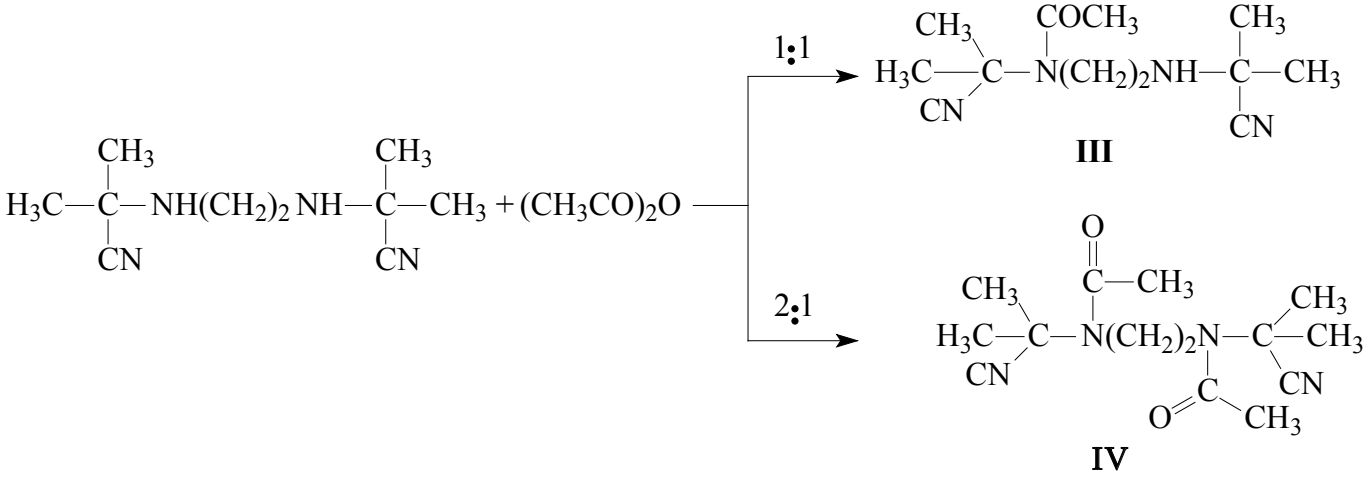

The results of the study of the primary biological activity of the compound N, N'-bis-(*α*-cyanisopropyl) ethylenediamine showed that it has a high stimulatory property. In order to obtain new biological active derivatives, we studied the reactions of N, N'-bis-(*α*-cyanizopropyl)ethylenediamine with various acid anhydrides. It should be noted that the structure of the compound formed

by the reactions of N, N'-bis-(α-cyanisopropyl)ethylenediamine with acid anhydrides depends on the mole ratio of the reacting compounds.

It was observed that N-monoacyl product is formed as a reaction product when reactive reagents are used in the ratio of 1: 1 mol, and bis-acyl product is formed when the reaction is carried out in the ratio of 2: 1 mol. In studying the reactions of N, N'-bis-(α-cyanisopropyl)ethylenediamine with acid anhydrides, we used acetic acid anhydride as the anhydride. Therefore, the formation of N-monoacetyl-N, N'-bis-(α-cyanisopropyl) ethylenediamine (II) as a reaction product was observed. When using reactive reagents in a ratio of 1: 2 moles, the formation of bis-acetyl product N, N'-diacetyl-N, N'-bis-(α-cyanisopropyl)ethylenediamine (III) as a reaction product was observed. In both cases, the reaction was carried out at the boiling temperature of the reaction mixture (solvent).

In the study of the reactions of aromatic acid anhydrides of N, N'-bis-(α-cyanisopropyl) ethylenediamine, we used benzoic acid anhydride as an aromatic acid. The reaction was carried out under the same conditions as with acetic acid anhydride, and it was found that with high yields (77%) N-monobenzoyl-N, N'-bis- (α-cyanisopropyl)ethylenediamine was formed (Table 1).

Table 1.– Physicochemical characteristics of mono- and bis-acyl products of some α-aminonitriles

Compounds	Ratio,%	T_m, melting point, °C	R_f	Molecular weight	Brutto formula
III	75	162–164	0.65	236	$C_{12}H_{20}N_4O$
IV	80	174–175	0.78	278	$C_{14}H_{22}N_4O_2$
V	77	150–152	0.46	298	$C_{17}H_{22}N_4O$
VI	82	245–247	0.38	402	$C_{24}H_{26}N_4O_2$

When using reactive reagents in a ratio of 1: 2 moles, the formation of N, N'-dibenzoil-N, N'-bis-(α-cyanisopropyl)ethylenediamine (VI) in high yields as a reaction product was observed.

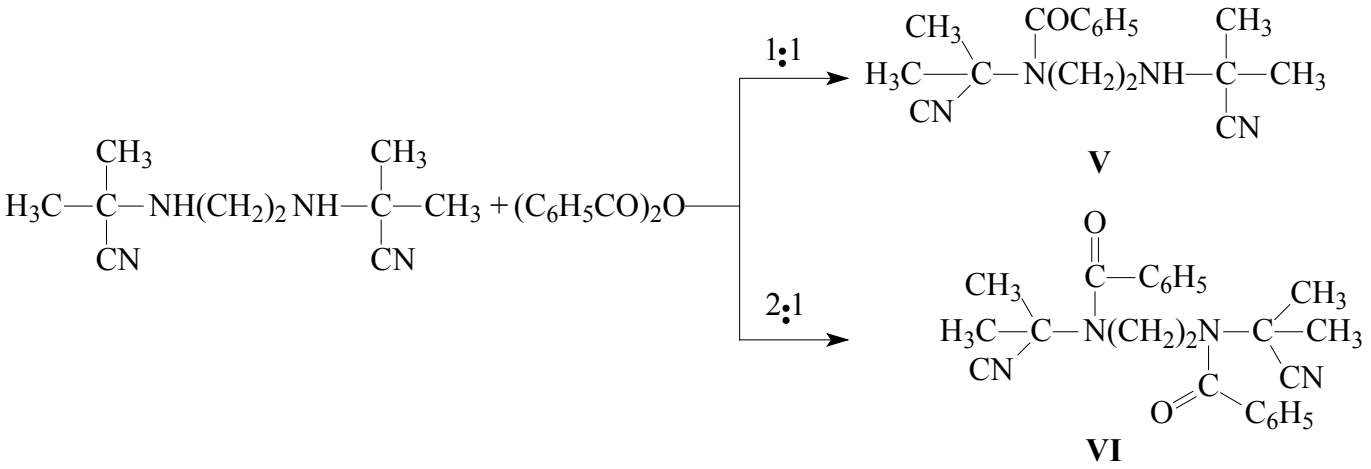

Thus, it was observed that the reactions of N, N'-dibenzoil-N, N'-bis-(α-cyanisopropyl)ethylenediamine with acid anhydrides (vinegar and benzoic acid) proceed under harsh conditions relative to monoamines. This situation is explained by the low degree of basicity of the secondary amino group in the bird state relative to the nitrile group relative to the free amino group, as well as the high CN-group. Therefore, the mono- and diacylation reactions take place under the same conditions, and it was found that the direction of the reaction depends on the mole ratio of the reacting aminonitrile-anhydride reagents.

Materials and methods

In that investigation we used by organic synthesis methods, various analytical observation methods, IR-, Mass- spectral and modern X-Ray crystallographic methods. We studied their structure by X-ray structural analysis in order to analyze the relationship between the structure and chemical properties of some of the α-aminonitrile derivatives obtained [5–6]. One of these substances, N, N-bis-(α-cyanisopropyl) ethylenediamine crystallizes in a triclinic spatial group with a center of symmetry. The asymmetrical part of a crystal cell consists of a single molecule. Although the molecule is symmetrically symmetrical, no symmetry is observed in its spatial structure in the crystalline state.

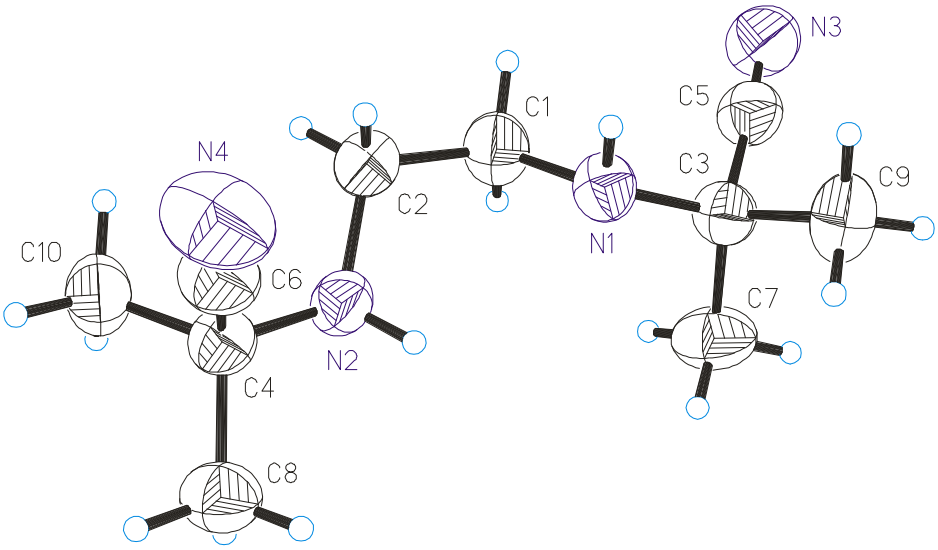

Figure 1. Spatial structure of N, N-bis-(a-cyanisopropyl)ethylenediamine molecule

In the molecule, the amino-group nitrogen atoms are in the sr3 hybrid state, and their configurations are reflected relative to the mutual plane. The lengths of the bonds in the molecule correspond to the average statistical values. The garden lengths are given in Table 1. The spatial structure of the molecule is shown in Figure 1. Analysis of intermolecular interactions shows that molecular dimers were formed in the crystal by means of a pair of symmetrical hydrogen bonds of the NH… NC type (Fig. 2).

Elemental cell parameters and diffracted X-ray intensities were determined on a CCD Xcalibur Ruby (Oxford diffraction) diffractometer. The crystallographic computer program SHELXTL was used to find the structure of the compound. The crystal cell parameters and calculation results are given in (Table 2).

Table 2.– Bond lengths (Å) obtained by X-Ray crystallographic method

Bonds	Length, Å	**Bonds**	Length, Å
N1–C3	1.456 (3)	**C3–C5**	1.488 (4)
N1–C1	1.469 (4)	**C3–C7**	1.526 (4)
N2–C4	1.455 (4)	**C3–C9**	1.536 (4)
N2–C2	1.457 (4)	**C4–C6**	1.499 (4)
N3–C5	1.141 (4)	**C4–C10**	1.516 (4)
N4–C6	1.135 (4)	**C4–C8**	1.524 (4)
C1–C2	1.515 (4)		

The geometry of the hydrogen bond is as follows: N1 – H1 0.85 (3) Å N1 – H1 … N4 2.46 (3) Å N1 … N4 3.290 (4) Å N1 H1 N4 angle 169 (3) °.

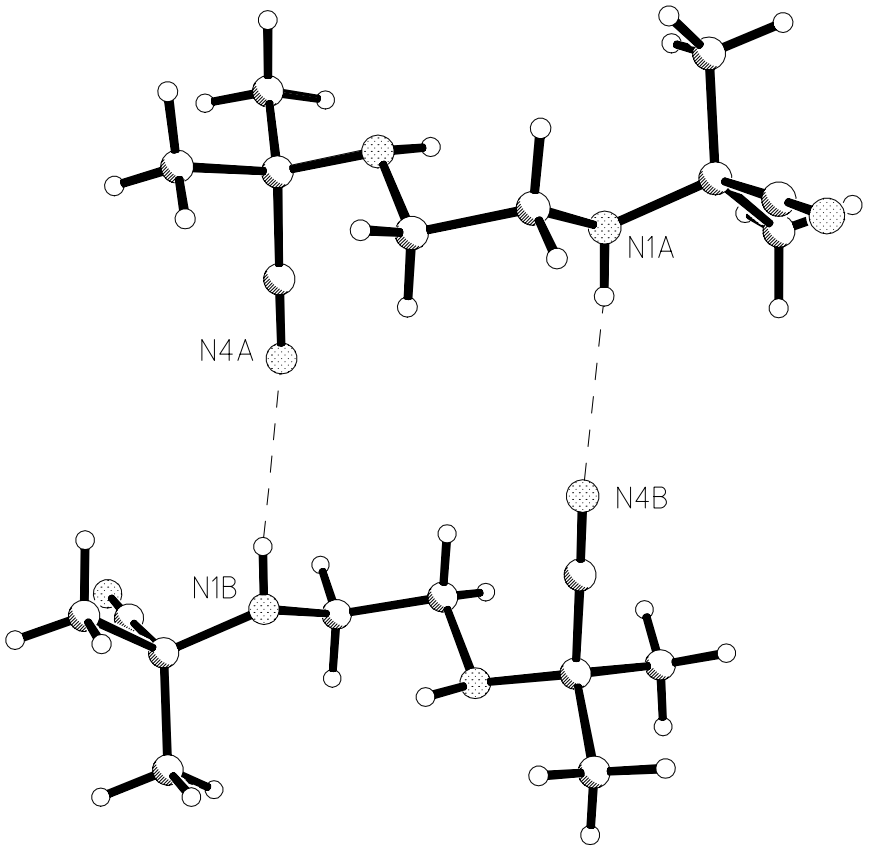

Figure 2. Intermolecular hydrogen bonding in a crystal

X-ray structural experiment. X-ray diffraction analysis showed that the crystals of the substance were grown at room temperature from a solution of N, N-bis-(α-cyanisopropyl)ethylenediamine. The results show that α-aminonitriles have the ability to form complex compounds with various biometals. They can also form both intramolecular and intermolecular complexes [7–8].

Results

Various functional groups were obtained by IR-spektral method. In the mass spectra of these compounds, the presence of high percentages of the peak corresponding to the molecular ion intensity of the compounds was observed. Elemental cell parameters and diffracted X-ray intensities were determined on a CCD Xcalibur Ruby (Oxford diffraction) diffractometer. The crystallographic computer program SHELXTL was used to find the structure of the compound.

Classification on base on chemical composition

α-Aminonitriles and their derivatives are listed as organic compounds in Section VI of the NGFEA. The following new brand codes have been proposed for the compounds of α-aminonitriles and their derivatives studied by us. Code number 292690950 1 for α-aminonitrile derivatives according to the nomenclature of goods in foreign economic activity (NGFEA) was recommended.

Proposed code numbers for α-aminonitriles and their derivatives

2926	The compounds contain a functional group of nitrile
292690950 0	others
292690950 1	α-aminonitriles and their derivatives
292690950 9	others

Conclusion

New α-aminonitrile derivatives synthesized and studied by modern physicochemical research methods. Products of reaction classified according to their chemical composition and obtained the digital product code.

Acnowledgments

The authors would like to thank Bakhtiyorjon Abduganiev, Colonel of the Customs Service of Uzbekistan, PhD in Chemistry, Associate Professor, for his assistance in the implementation of the product codes.

References:

1. Chuliyev J. R., Yusupova F. Z., Qosimova K. I., Kodirov A. A. Synthesis of some a-aminonitriles // Universum: Chemistry and Biology 2019. – No. 3 (57). P.– 61–64.
2. Kodirov A. A., Shodiyev G. Ch., Ergasheva R. U., Meyliyeva M. Study of a-aminonitrile acylation and benzoylation reactions // QarSU news 1/2017. – P. 32–34.
3. Chuliyev J. R., Norboyeva G. B., Kodirov A. A., Mamarakhmonov M. Kh., Askarov I. R. Reactions of a-aminonitrilov atsilirovaniya // Universum: Chemistry and Biology. 2019. – No. 9(63).– P. 34–37.
4. Chuliyev J. R., Yusupova F. Z., Kodirov AA.A., Mamarakhmonov M. Kh., Askarov I. R. Study of benzolination reactions of α-aminonitriles Universum: Chemistry and Biology 2019. № 11 (65).– P. 62–64.
5. Chuliyev J. R., Kodirov A. A., Mukarramov N. I. Acylation and benzoylation reactions of α-aminonitriles, XIII International Symposium on the Chemistry of Compounds. Shanghai. October 16–19. 2019. – 83 p.
6. Chuliyev J. R., Yusupova F. Z., A. A. Kodirov E. T. Berdimurodov, K. K. Turg‘unov Synthesis, X-Ray Characterization, IR Vibrational Frequencies, NMR Chemical Shiftsand DFT Propertiesof 2, 7-Dimethyl-2, 7-Dicyanide-3, 6-Diazaoctane. International Journal of Innovative Technology and Exploring Engineering (IJITEE) Volume-9 Issue-3, January, 2020. – P. 396–404.
7. Kodirov A. A. To study the reactions of acetontsyanhydrin with various amines // News of the National University of Uzbekistan 2017. – No. 3/2. – P. 422–424.
8. Chuliyev J. R., NNaimov Kh. A., Norboyeva G. B., Kodirov A. A. The study the acylation and benzoylation reactions of α-aminonitriles. QarSU news 4/2019. – P. 17–21.

Contents